CHEMOSTRATIGRAPHY AND THE PALEOCEANOGRAPHY OF THE BOSSIER-HAYNESVILLE FORMATION, EAST TEXAS BASIN, TX AND LA, USA

by

PUKAR MAINALI

Presented to the Faculty of the Graduate School of

The University of Texas at Arlington in Partial Fulfillment

of the Requirements

for the Degree of

MASTER OF SCIENCE IN GEOLOGY

THE UNIVERSITY OF TEXAS AT ARLINGTON

December 2011

ACKNOWLEDGEMENTS

I would like to thank my advisor, Dr. Harold Rowe, for his time and energy, and for the guidance throughout graduate school. I would like to thank Dr. Stephen Ruppel, and Dr. Ursula Hammes of the Texas Bureau of Economic Geology, Jacksons School of Geoscience (UT Austin), for providing access to the cores, and for their help throughout this project. I would like to thank James Donnelly, Nathan Ivicic, Kenneth Edwards and Josh Lambert for their help in handling cores. I want to thank my committee members Dr. Andrew Hunt and Dr. Wickham for their support for the project. I want to thank Dr. John Holbrook and Ron Tingook for their thoughts and conversations on sequence stratigraphy. I want to thank Dr. Chris Scotese for providing the paloegeographic maps. I cannot forget to thank the geochemistry research group at UT Arlington for their help. I want to thank Niki Hughes, James Hoelke, and Jak Kearns for assistance and discussions on geochemistry. Niki and Kyrstin Robinson for help with calibration of the instrument, Rob Nikirk, Nidal Jabri and Karen McCreight for lab help.

I would also like to thank UT Arlington Geoscience Department for two years of grad-school support.

November 21, 2011

ABSTRACT

CHEMOSTRATIGRAPHY AND THE PALEOCEANOGRAPHY OF

THE BOSSIER-HAYNESVILLE FORMATION,

EAST TEXAS BASIN, TX AND LA,

USA

Pukar Mainali, M.S. Geology

The University of Texas at Arlington, 2011

Supervising Professor: Dr. Harold Rowe

The fine-grained, dark, organic, calcareous Haynesville shale (Kimmeridgian) and the overlying carbonate-poor Bossier shale (Tithonian) were deposited during the warmer Jurassic period in the tectonically formed East Texas Basin. Thirteen drill cores recovered from six counties (Texas) and four parishes (Louisiana) have been studied for their geochemistry. Each core was analyzed at a 1-foot interval using a handheld x-ray fluorescence instrument, providing rapid, quantitative analysis of the following elemental concentrations: Mg, Al, S, Si, P, K, Ti, Ca, Mn, Fe, Mo, Cr, Ni, Cu, Zn, Th, Rb, U, Sr, Zr, and V. In addition, XRD analyses (10 samples from T.W. George), TIC, TOC, %N, and C and N isotopes were generated and integrated in the study. Mineralogical and major elemental geochemistry (e.g. Si/Al) suggests a carbonate-rich Haynesville mudrock coarsening up into siliciclastic dominated Bossier formation. Trace elements (enrichment of Mo (ppm) and Cr/V, Mo-TOC and Fe-S-TOC relationships indicate anoxic-euxinic bottom water conditions turned dysoxic-oxic during the course of Haynesville-

Bossier deposition and a deep-water renewal time ~100 years. The provenance of organic matter was determined to be of lacustrine-marine algae for the Bossier, and of terrestrial plants for the Haynesville shale, based on the C/N ratios. Furthermore, an attempt was made to associate the geochemical transgressive-regressive cycles observed in the Bossier-Haynesville to the global 2nd order sequence, and the more local 3rd order sequence stratigraphic surfaces observed in the GOM.

TABLE OF CONTENTS

LIST OF ILLUSTRATIONS

LIST OF TABLES

CHAPTER 1

INTRODUCTION

1.1 Project Outline

Black shales are organic-rich, fine-grained deposits, which typically accumulate under anoxic-euxinic, deep-water basinal locations (Demiason and Moore, 1980, Wignall and Maynard, 1993, Wignall and Newton, 2000). The hydrocarbon reservoir potential of these black shales has been recognized, and dates back at least a century ago when Pompeckj in his 1901 paper regarded organic rich shale from euxinic environments as a potential source rock (Brumsack, 2006). With advances in science, and new drilling and completion technologies (Steinhoff, et.al, 2011), stimulated by the ever soaring price of energy, black shales have evolved to be a major source for hydrocarbon deposits. Additionally, the presence of a variety of other toxic trace elements makes black shale study of economic and environmental importance (Piper and Calvert, 2009). Mudrocks are also of great academic interest, because they constitute an estimated two third of the sedimentary record (Schieber and Zimmerle, 1998), and as a result preserve a significant amount of the Earth's history.

The organic-rich Jurassic Bossier and Haynesville (B-H) Formations of East Texas and western Louisiana (**Figures 1.1 and 1.2**) are interpreted to represent organic-rich, fine-grained deposition on a gently dipping ramp (Ahr, 1973; Faucette and Ahr, 1984), or in a intraplatform basin in the north and a distally steepened ramp in the south (Hammes et al., 2011), after separation of North America from Gondwana during the mid-Mesozoic (**Figure 1.3**; Scotese, PALEOMAP Project).

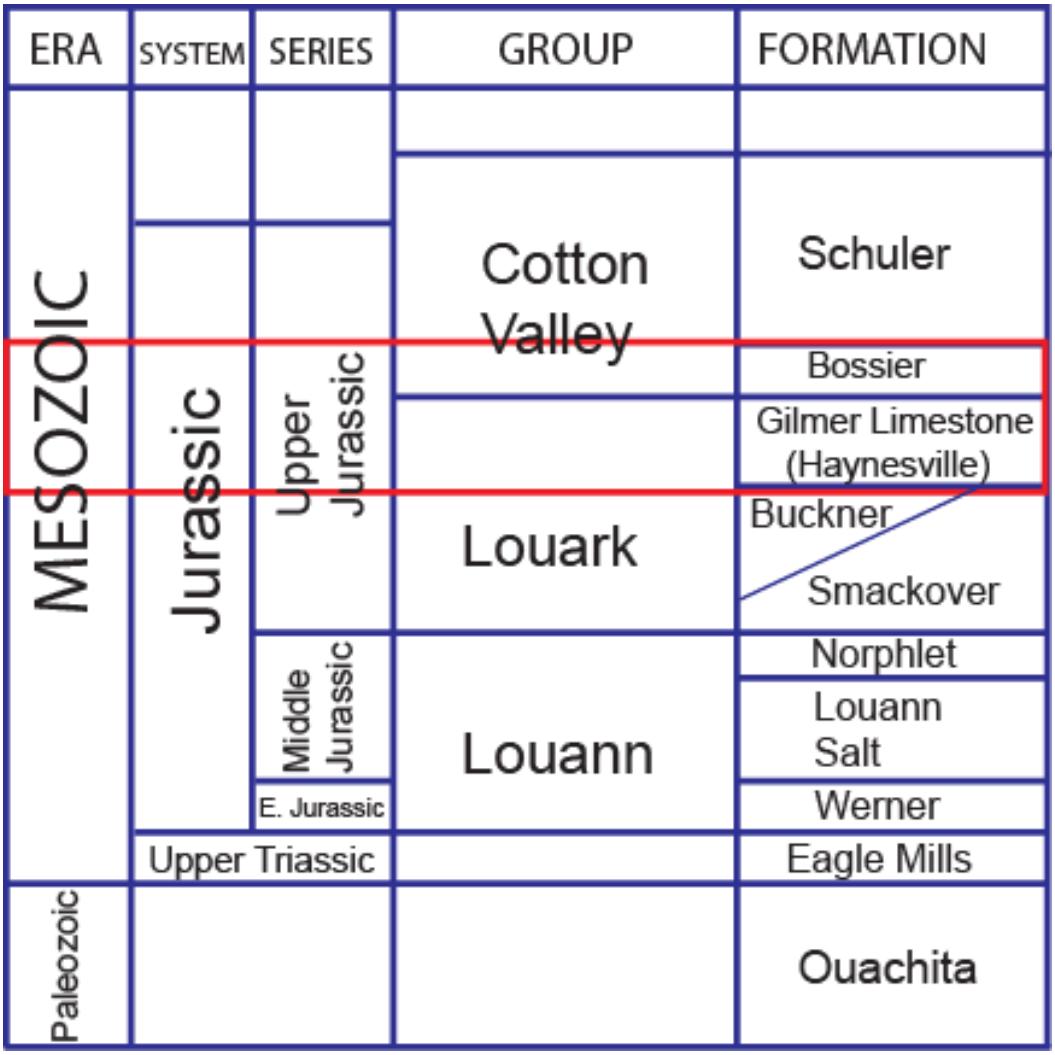

Figure 1.1 Timescale for Jurassic of the East Texas Basin (from McGowen and Harris, 1984).

Regionally, the Tithonian-aged Bossier and the Kimmeridgian-aged Haynesville is a dark, organic rich, argillaceous, silty, calcareous mudstone deposited in the East Texas Basin between approximately 156 and 145.5 million years ago during the Jurassic period (Spain and Anderson,2010;Hammes,2009). The Haynesville is significantly more calcareous than the

overlying Bossier, and is notably less calcareous than the underlying Smackover Formation of mid-Jurassic age. Both Bossier and Haynesville are characterized by very low permeability but high porosity compared to other shales. The Haynesville Shale is interpreted as a continuation of the transgressive Gilmer Lime carbonates (Goldhammer, 1998), and includes marly laminated dark mudstone in the intrashelfal sub-basin, and high-energy carbonates in the proximal areas (Steinhoff et.al. 2011). Though both shales are prospective for shale-gas production, the Haynesville is more organic carbon rich, whereas the Bossier is more clay rich (Cicero et al., 2010; Hammes, et al., 2011).

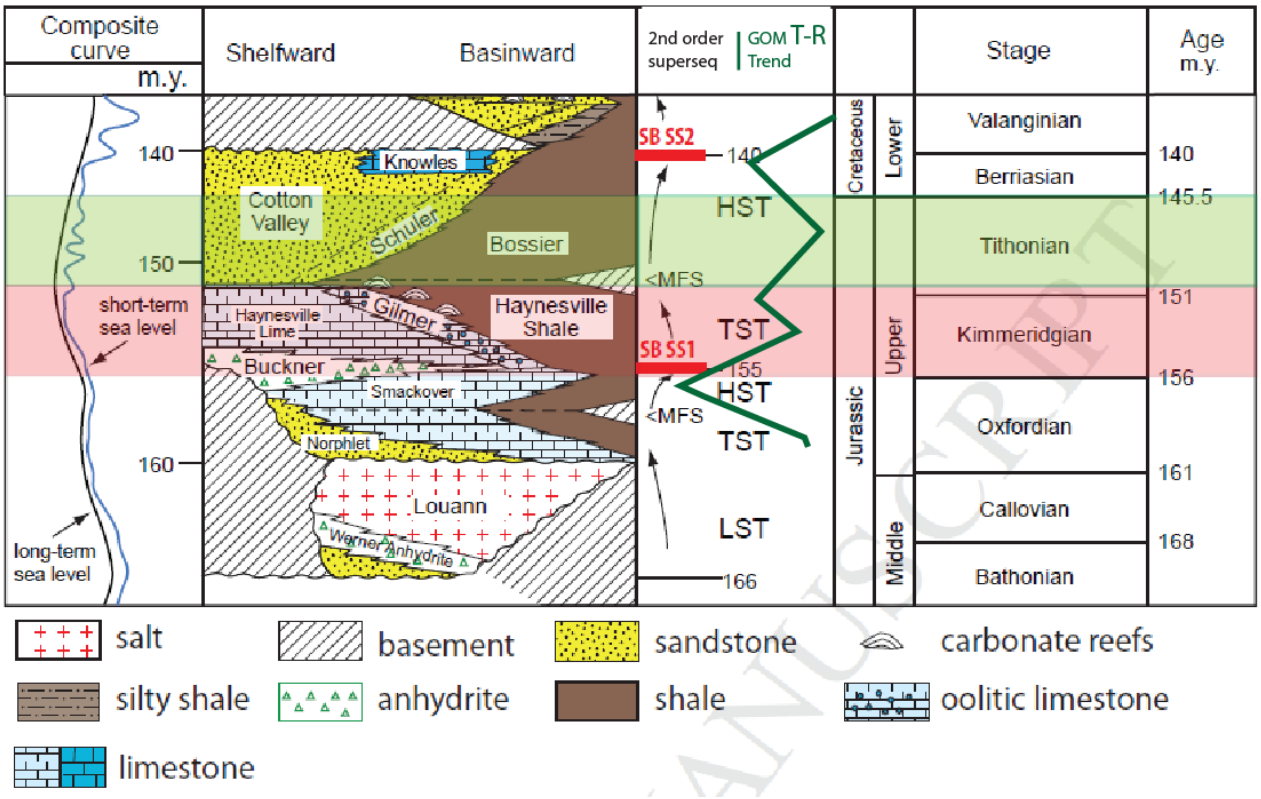

Figure 1.2 Stratigraphy of East-Texas Basin, and transgressive-regressive sequences of the Jurassic section of Northwestern Gulf of Mexico. (after Goldhammer, 1998, 1998; Mancini et. al., 2004; Hammes et al, 2011).

Haynesville production estimated at over 3 TCF (trillion cubic feet of gas) and 181 MMBO (million barrel of oil) (Ewing, 2001), continues to be an active target for shale gas in the Texas-Louisiana region.

1.2 Geologic Setting

The study area, the East Texas Basin (ETB) (**Figure 1.4**) is in the NW Gulf of Mexico (GOM) Basin (Jackson and Lauback, 1988), and is recognized as a sub-basin, or extension of the larger Gulf of Mexico Basin (Wood and Walper, 1974; McGowan and Harris, 1984; Salvador, 1991). Triassic rifting along the back of the Ouachita thrust belt that continued throughout the Jurassic, accompanied by breakup, rifting and extension of Pangea, sea-floor spreading and migration of various cooling and thermally subsiding lithospheres led to the formation of the Gulf of Mexico Basin (Pindell and Dewey, 1982; Nunn, J.A., 1984; Nunn et.al., 1984; Jackson and Laubach, 1988; Salvador, 1987; Goldhammer and Johnson, 1999; Mancini et al., 1999; Marton and Buffler, 1999; Pindell and Kennan, 2009, Steinhoff et.al, 2011).

Most researchers agree that the East Texas Basin developed within either megashear zones or rift grabens or aulacogens that formed along the margin of the Gulf of Mexico, probably corresponding to the breakup of Pangea and the separation of North and South Americas during the Triassic (Kehle, 1971; Burke and Dewey, 1973; Moore et al., 1974; Wood and Walper, 1974; Beall, 1975; McGowen and Harris, 1984). However, a recent study suggests that the Gulf of Mexico was a back-arc basin (Stern and Dickinson, 2010). It is yet unclear how the East Texas Basin fits into this newly-hypothesized geometry for the greater Gulf of Mexico.

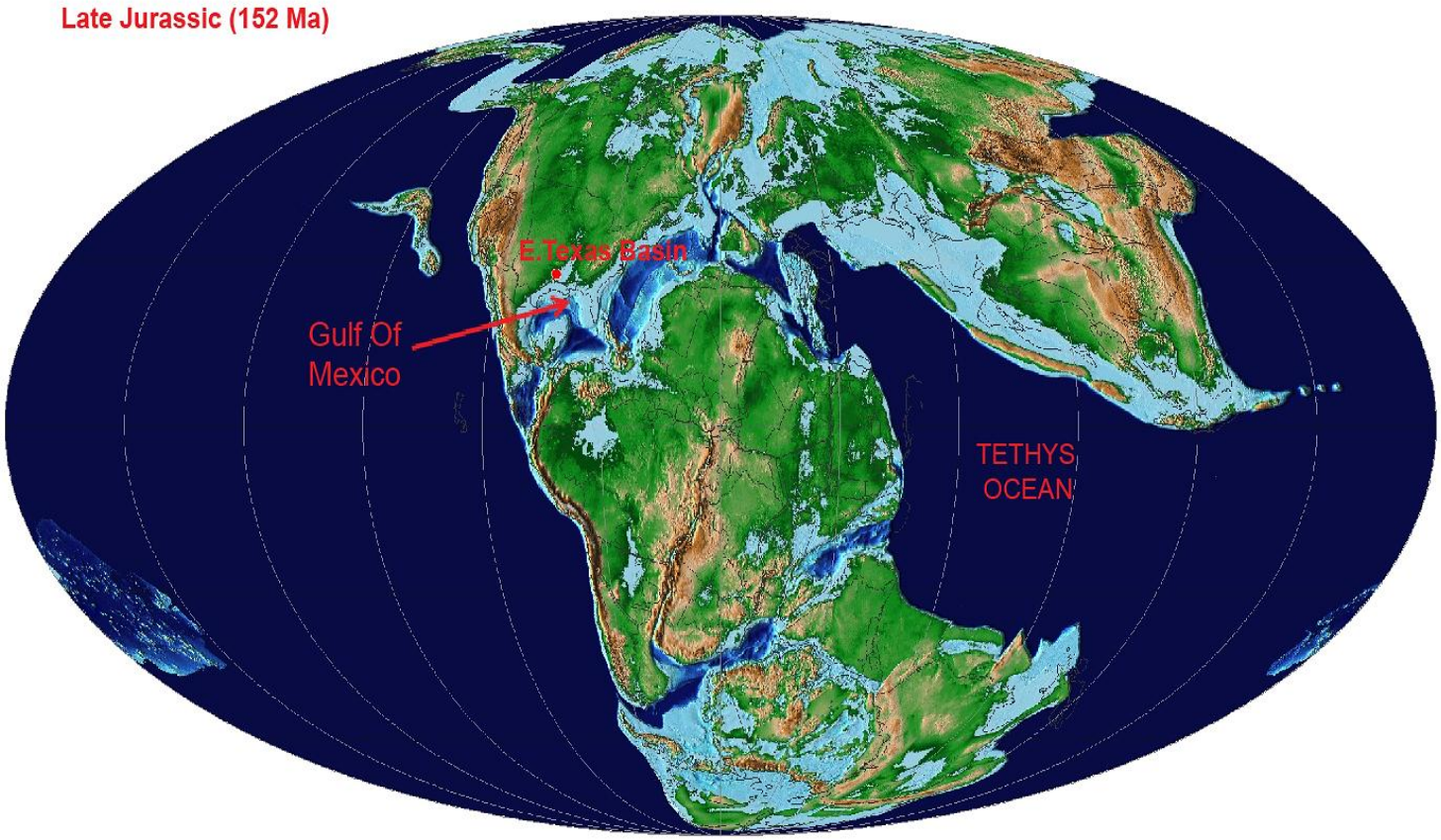

Figure 1.3 Kimmeridgian Gulf of Mexico, Paleogeographic maps by C.R. Scotese, Paleomap Project (www.scotese.com).

The mid-Jurassic to the upper-Cretaceous tectonic evolution of the East Texas Basin is dominated by divergent margin development associated with the opening of the Gulf of Mexico province (Salvador, 1987; Goldhammer and Johnson, 1999; Marton and Buffler, 1999), and the stratigraphic evolution is dominated by eustacy (Todd and Mitchum, 1977; Vail et.al., 1984; Haq et al., 1987), largely controlled by plate tectonics (Hallam, 2001).

A possible elevated southern margin of the East Texas Basin could have restricted the water circulation between the Basin and the Gulf of Mexico, precipitating the Werner Anhydrite and the Louann Salt in the early Jurassic. Continued subsidence is suggested to have resulted in open marine conditions, evidence of which is the occurrence of the carbonate-rich Smackover and the Haynesville (Gilmer) Formation (McGowen and Harris, 1984).

The study area lies within the interior zone of the Gulf of Mexico Basin (Ewing, 1991). Within this zone are the Northern Louisiana Salt Basin separated from the Texas Basin by the pre-Smackover Sabine uplift (Ewing, 2001), and the Mississippi basin separated from the Louisiana Basin by the Monroe uplift (Lowrie et. al, 1993). The East Texas Basin is quite comparable in size to the North Louisiana Salt Basin, about 125 to 150 km long and about 50 km wide, but the central Mississippi basin is several times larger (Lowrie et. al, 1993).

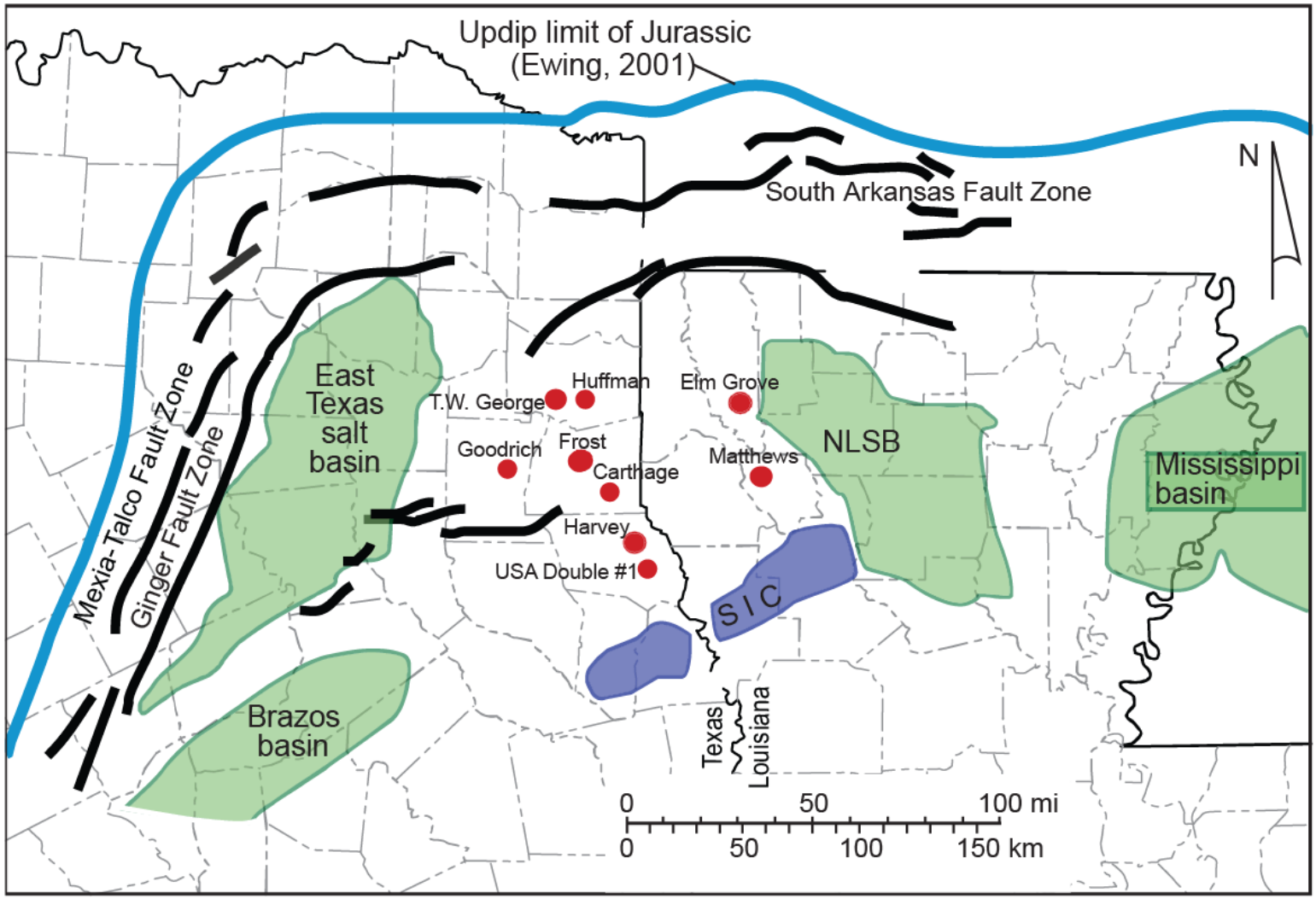

Figure 1.4 Map of study area, core names and the locations of the cores analyzed in the study in the East Texas Basin.

The basinal bathymetry, carbonate platforms and salt movement associated with the opening of the Gulf of Mexico Basin immensely influenced the Bossier-Haynesville deposition (Hammes and Frebourg, 2011). Stratigraphically, the fluvial and eolian siliciclastic Norphlet formation advanced basin-ward (Steinhoff et. al, 2011), following the Callovian-aged (Salvador, 1991) Louann Salt, deposited after the initial rifting, and sits atop the salt. Overlying the siliciclastic Norphlet is the late Jurassic (Oxfordian-Kimmeridgian) marine carbonate-rich Louark Group, composed of the Smackover, Buckner and Haynesville formations. Siliciclastic input into the basin during Haynesville deposition was mostly from the north and northeast, allowing carbonate facies development to the south and west (Goldhammer, 1998; Ewing, 2001; Hammes et al., 2011). Cessation of this carbonate deposition occurred in the Tithonian Early Cotton Valley Group with siliciclastic input from north, northeast and northwest.

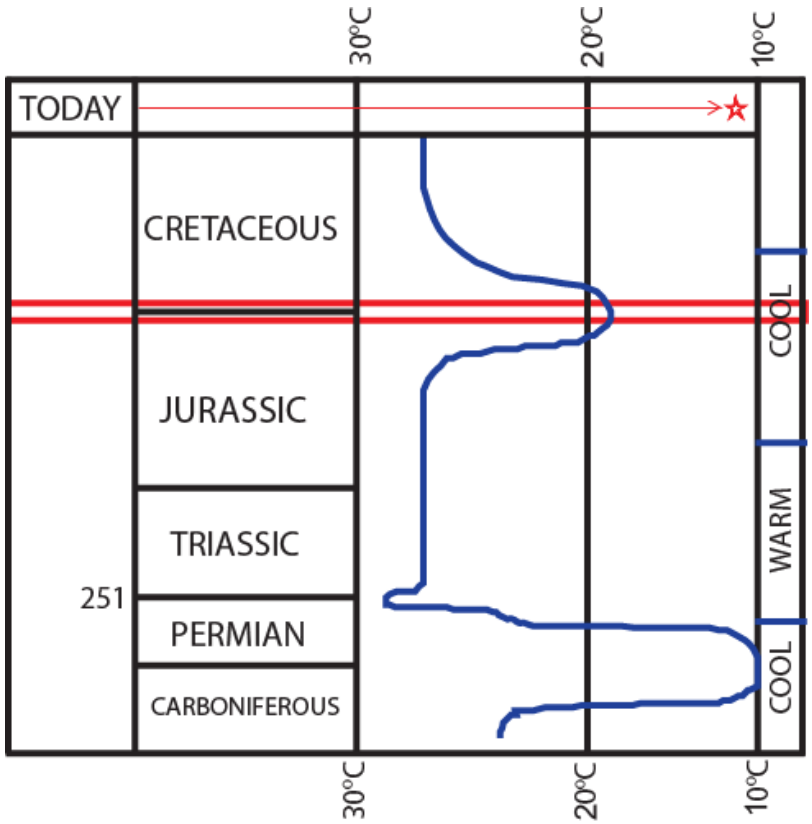

Figure 1.5 Global Climate change (Scotese et al.1999).

The general agreement on the Jurassic climate is that it was warmer than the present (**Figure 1.5**) without polar ice-caps (Hallam, 1985). A global change from a humid to a more arid climate has been suggested during the late Jurassic period (Schudack, 1998). The Bossier-Haynesville shale was deposited during a period worldwide transgression (Hallam, 1978, 2001, Goldhammer, 1999), with the maximum sea level rise (MFS) at the Tithonian Haynesville-Bossier boundary (Goldhammer, 1999; Hammes, 2009, 2011) that eventually fell in the Early Cretaceous (Haq et al., 1987; Hallam 1988). The lack of evidence for glacioeustacy during the late Jurassic (Jenkyns et al., 2011), indicates the involvement of plate tectonics for eustatic changes, especially affected by the opening of the Atlantic and the Indian oceans (Hallam, 2001). Moreover, increased volcanism leading to an elevated concentration of atmospheric carbon dioxide is suggested (Berner, 1994).

1.3 Study Objectives

The objective of the proposed research is to better understand the depositional environment of the Bossier and Haynesville Formations of the East Texas basin. Chemostratigraphy, the study of the variation of chemistry in sedimentary sequences, is utilized to meet this objective in this study. The geochemistry of sedimentary rocks is the result of their provenance, depositional setting, and the diagenetic history (Andrew et al., 1996), and such analyses of mudrocks are indispensable to be able to observe subtle differences during deposition (Algeo et al., 2003; Rimmer et al., 2004; Rowe et al., 2008). The study of the variations in major and trace element abundances in sedimentary rocks, chemostratigraphy utilizes the application of major and trace elements to characterize and sub-divide geochemically distinct units, for regional (or global) correlation of strata (Andrew et al., 1996). Major elements variations largely indicate changes in mineralogy, and are used to differentiate lithology changes in the stratigraphic zone, and thus can help in correlation. Redox-sensitive

elements which are generally considered syngenetic and can be more than a hundred times their crustal abundance in some black shale (Vine and Tourtelot, 1970), can aide in the reconstruction of the possible paleodepositional conditions of sedimentary rocks (Tribovillard et al., 2006).

A multi-proxy geochemical approach was chosen in this research, where Mo, DOP, Fe-S-TOC, V/Cr were used to assess redox conditions. Si, Zr, Ti were studied as proxies for clastic influx, and P fulfilled the role as a paleoproductivity indicator. Specifically, the study will focus on defining and refining the geochemical and sedimentological changes observed in the organic-rich strata of the Bossier and Haynesville Formations in the East Texas Basin. It is anticipated that the boundary between the Haynesville and the more siliciclastic Bossier Formation will be better defined.

CHAPTER 2

METHODS

2.1 Drill core information

Twelve drill cores of Kimmeridgian aged Haynesville formation (as shown in table 2.1), from six counties of Texas and two parishes from Louisiana were studied.

Table 2.1 Core Information

Core Name	**County / Parish**	**Location** (Latitude/ Longitude)	**API #**	**Samples / Length Analyzed**	**Slabbed**	**Ed-XRF Unit**
1.Davis Bros Core	Jackson Parish		1704920110	33 samples 31 feet		BEG
2.Frost 5-11	Panola County	32.16549/ - 94.18034	4236537169	274 samples 388 feet	Yes	BEG
3.Goodrich	Rusk County	32.18072/ -94.58642	4240134843	171 samples 188 feet	Yes	UTA 1
4.Harvey Core	Shelby County	31.84624/ -94.04811	4241931428	164 samples 171 feet	Yes	BEG
5.Jones Core	San Augustine County		4240530003	100 samples 176 feet		BEG
6.Temple #1	Sabine County	32.16509/ - 94.18163	4240330016	69 samples 67 feet	Yes	BEG
7. T.W George	Harrison County	32.40152 / -94.42797	4220334557	386 samples 467 feet	Yes	BEG
8.Carthage	Panola County	31.32908/ -93.79314	4236537151	301 samples 300 feet	Yes	BEG
9.Huffman No.1	Harrison County			272 samples 301 feet	Yes	UTA 1

Table 2.1- continued

10. Elm Grove	Bossier Parish		1701524392	164 samples 170 feet	Yes	UTA 1
Crown Zallerbach	Winn Parish		1712720820	20 samples 23 feet		BEG
12. Matthews	Red River Parish		1708120937	109 samples 130 feet	Yes	UTA 2
13. USA Double #1	Shelby County	31.716210/ -93.972310	4241931396	165 samples 301 feet	Yes	BEG (maj) UTA 1 (Tra)

2.2 Energy dispersive X-Ray Fluorescence (ED-XRF)

All cores were analyzed for inorganic elemental chemistry using a Bruker S1 Tracer III-V handheld energy dispersive X-ray fluorescence instrument at approximately one foot sampling interval. The unit was kept stationary and slabbed cores were analyzed for major and trace elements by placing a flat surface of the samples on the 3 X 4 mm window on the top of the instrument. A flat surface is necessary because the measurement sensitivity of the ED-XRF instrument is inversely proportional to the distance from the silicon detector (SiPIN), located directly below the sampling window (Hughes, 2011). Therefore, a Dremel with a tungsten carbide tip was used to create a flat surface whenever necessary.

Two separate data acquisitions were necessary for each sample, to measure major and trace elements. Major element data collection was conducted at 15Kv for a count time of three minutes in a vacuum pumped instrument with the vacuum reading less than 2 Torr. The Vacuum pump was used to remove air between the sampling window and the detector. Trace elemental analyses were conducted at 40Kv for a count time of 3 minutes in a filtered instrument setting. The filter was used to prevent low-energy s-rays from reaching the detector.

Both major and trace element analysis was undertaken at the same location on the core face, marked by a white out fluid or a sticker with sample number on it.

2.2.1 Calibration of Ed-XRF

Calibration of major and trace element measurement of mudrocks was undertaken using a suite of ninety reference materials (Rowe and Hughes, 2010)

The ninety standards are-

5 Internationally accepted standards

7 from the Devonian-Mississippian Ohio shale

20 from the Pennsylvanian Smithwick formation of central Texas

27 from the Devonian- Mississippian Woodford formation of west Texas

15 from the late Cretaceous Eagleford formation of south Texas

16 from the Mississippian Barnett formation of north- central Texas

Each of the ninety reference materials was pressed in a Carver press to forty tons with a forty millimeter die using a boric acid backing. Each reference material was pulverized to approximately 8 grams of 200 mesh powder using a TM Engineering pulverizer with trace metal grade stainless steel pulverizing cups and pucks. Approximately eight grams of powdered reference material were used in each reference material.

For calibration, each pressed pellet was analyzed three times each for a count time of six minutes for both major and trace elements at different locations on the pellet face. The voltage was consistent for the different instruments. However, due to the inter-instrument variance caused by the differences in manufacturing, the analyzing current varies between each instrument.

All of the two hundred and seventy major element X-ray spectra (90 references X 3 analysis each) were loaded into the Bruker CalProcess software along with a reference table with known accepted elemental concentration values for each element. For each element, slope and background inter-element correction was performed. During the calibration all the samples that did not fall within the ninety-five percent confidence interval were deleted and unfit element spectra were omitted from the calibration. A second round of calibration was performed once the initial calibration curves were analyzed, and statistical analysis of each element calibration curve was performed. A similar process was performed for trace elements. Major element calibration encompasses the following elements: Magnesium, Aluminium, Silicon, Phosphorus, Sulfur, Potassium, Calcium, Titanium, Vanadium and Chromium. Trace element calibration encompasses the following elements: Cobalt, Nickel, Copper, Zinc, Thorium, Rubidium, Uranium, Strontium, Zirconium and Molybdenum. A more detailed evaluation of this calibration process can be found in Rowe and Hughes in prep. Raw spectra from unknowns are processed through a calibration spreadsheet. For major element analysis no filter was used, but a Al-Ti-Cu filter was used for trace element analysis.

2.3 Additional Lab Analysis (LECO-S, TIC, TOC, $\delta^{13}C$, and $\delta^{15}N$)

2.3.1 Sample Preparation

Samples for additional analyses were either collected by directly drilling powder off the back of the core or the edge of the face of the analyzed location or by cutting discrete samples off the back of the cores using a standard rock saw and subsequently pulverizing them by the TM Engineering Pulverizer. The pulverized samples taken directly from the core were pulverized/drilled using a Foredom Drimmel with a tungsten carbide drill, and stored in a micro

centrifuge tube (BWR-20170-293). When samples were collected, they were subsequently pulverized using a TM Engineering pulverizer with trace metal grade stainless steel pulverizing cups and pucks. The samples were then placed in standard plastic liquid sample cups. Samples were weighed out into the appropriate container prior to analysis.

2.3.2 Total Inorganic Carbon (TIC)

Samples were analyzed at the University of Texas at Arlington for their total inorganic carbon (TIC) content using a UIC, Inc. coulometer equipped with a CM5230 acidification module with average unknown standard deviations of less than 0.5 percent (Engleman et al 1985). For TIC analysis, weighed samples are acidified at high temperature with ten (10) percent phosphoric acid (H_3PO_4). A Baker analyzed $CaCO_3$ check standard was used.

2.3.3 TOC/TN/Carbon Isotopes/Nitrogen Isotopes

Total organic carbon (TOC), total nitrogen (TN), and stable isotopic compositions of TOC ($\delta^{13}C$) and TN ($\delta^{15}N$) were performed on powdered samples that were weighed into silver capsules (Costech Analytical, Inc. #41067) and subsequently acidified repeatedly with 6% sulfurous acid (H_2SO_3) in order to remove carbonate phases (Verardo et al., 1990). Samples were analyzed at the University of Texas at Arlington using a Costech 4010 elemental analyzer interfaced with a Thermo Finnigan Conflo IV device to a Thermo Finnigan Delta-V isotopic ratio mass spectrometer (IRMS). Isotopic results are reported in per mil (‰) relative to V-PDB for $\delta^{13}C$ and air for $\delta^{15}N$. The average standard deviations were 0.11‰ and 0.07‰ for $\delta^{13}C$ and $\delta^{15}N$ of USGS-40 glutamic acid (IAEA-8573), respectively. The average standard deviations for

unknown samples analyzed in triplicate were <0.1‰ for $\delta^{13}C$ and $\delta^{15}N$, 0.02% for TOC, and 0.01% for TN.

2.3.4 LECO Sulfur

Sulfur analyses were conducted using a LECO C-S analyzer, with the standard deviation of unknowns averaging less than 0.01%. A subset of samples was analyzed for sulfur using the LECO Sulfur method (Table 2.2).

2.3.5 XRD

Samples were analyzed by the powder X-ray diffraction method at the Kentucky Geological Survey using a Bruker D8 X-ray diffractometer (see Table 2.2). XRD spectra were collected using copper radiation. Both unglycolated and glycolated clay fractions were prepared and analyzed across the 2Θ angular range (2 to 22^{o}) using a suspension and powder peel method across the 2Θ angular range of (2 to 90^{o}).

Table 2.2 Number of samples analyzed by type per core

Core Name	ED-XRF	(TIC)	(TOC)	Total Percent Nitrogen (TN)	Carbon Isotopes	Nitrogen Isotopes	Percent Sulfur (LECO)	X-Ray Diffraction (XRD)
1.Davis Bros	**33**	**-**	**-**	**-**	**-**	**-**	**-**	**-**
2.Frost 5-11	**274**	**-**	**-**	**-**	**-**	**-**	**-**	**-**
3.Goodrich	**171**	**-**	**-**	**-**	**-**	**-**	**-**	**-**
4.Harvey	**164**	**-**	**-**	**-**	**-**	**-**	**-**	**-**
5.Jones Core	**100**	**-**	**-**	**-**	**-**	**-**	**-**	**-**
6.Temple #1	**69**	**-**	**-**	**-**	**-**	**-**	**-**	**-**
7. T.W George	**386**		**126**	**126**	**126**	**126**	**-**	**10**
8.Carthage	**301**	**300**	**300**	**300**	**300**	**300**	**-**	**-**
9.Huffman No.1	**272**	**-**	**-**	**-**	**-**	**-**	**-**	**-**
10. Elm Grove	**164**		**158**	**158**	**158**	**158**	**164**	**-**
11. Crown Zallerbach	**20**	**-**	**-**	**-**	**-**	**-**	**-**	**-**
12. Matthews	**109**		**98**	**98**	**98**	**98**	**-**	**-**
13. USA Double #1	**165**		**143**	**143**	**143**	**143**	**-**	**-**

CHAPTER 3

RESULTS

X-ray diffraction (XRD) results from the T.W. George core (Harrison County, TX), LECO-Sulfur of the Elm Grove Core (Bossier Parish, LA), total inorganic carbon (TIC) of Carthage core (Panola County, TX), and the results from a total of nine cores listed in tables 3.1, 3.2 and 3.3 have been used for interpretation in the study. More focus has been given to the T.W. George and Huffman cores (both from Harrison County, TX), and the Elm Grove core (Bossier Parish, LA) to represent the western and eastern East Texas Basin respectively. This was possible due to the similar XRF results generated from other drill cores, which could be spatially divided into either eastern or western, and be interpreted similarly. The core chemostratigraphy has been divided into at least three packets, (top, mid and bottom are color coded in the figures) by variations observed in major elements Ca, Si and Al, that differentiate the lithology of the rock.

Graphs in this section contain the result from X-ray fluorescence spectrometry and other geochemical analyses described in the methods section. All plots have units in weight percent (e.g. % Ca) for major elements, parts per million (ppm) for trace elements (e.g. Zn (ppm), degree of pyritization (DOP_T), per mil ($^o/_{oo}$), whole number ratio (C/N), or are expressed as enrichment factors (EF).

3.1 X-Ray Diffraction (XRD)

Four Bossier samples, and six Haynesville samples were picked due to their elemental variability observed with the XRF from the T.W. George core, and were analyzed for mineralogy using XRD at the University of Kentucky **(figure 3.1**). The T.W. George core is assumed to reflect the mineralogy of other Bossier-Haynesville core from ETB. The XRD result indicates a more calcitic Haynesville with overall high quartz (though slightly higher in the Bossier) accordant with values generated with the XRF as in **Figure 3.2** which are the XRF generated chemostratigraphy of the same core.

3.2 Core Chemostratigraphy

3.2.1 Detrital Fraction

Figure 3.2 shows the percent elemental chemostratigraphy of the major elements (Si, Ca, K, and Fe) detrital indicators (Ti, Zi), and anoxia/euxinia indicator (Mo) of the T.W. George core. The boundary between the Bossier and the Haynesville Shale is observed at 11,100 feet (3383.28 meters) by a distinct downward increase in % Ca and a slight decrease in % Si in the T.W. George core. Similarly, the Bossier-Haynesville contact is picked at 10970.5 feet (3343.81 meters) and 10490 feet (3197.35 meters) for the Huffman and the Carthage cores respectively (chemostratigraphy not shown). The Haynesville is significantly more calcitic than the overlying Bossier. The Bossier has more detrital elements such as Ti and Zr compared to the underlying Haynesville, but has a significant decrease in Mo observed in the silty-mudstone of the Bossier formation.

Figure 3.3 shows cross-plots of detrital elements against Al (a proxy for clay). Si and Ti form good linear trends with Al in both the Bossier and the Haynesville shale. We witness the dominance of clay in the Bossier represented by higher concentrations of Al. Major elements

normalized to clay (Si/Al, Ca/Al, K/Al) detrital indicators normalized to clay (Ti/Al, Zi/Al), and anoxia indicator normalized to clay (Mo/Al and Fe/Al) of the Harvey Core is shown in **Figure 3.4**. Ratios of detrital elements like Si and Ti concentration to Al will "normalize" the element to clay (Tribovillard et al., 2006).Notice the abrupt increase in % Ca, and % TOC, and the decrease in Mo (ppm) in the lower Haynesville in the Harvey core **(figure 3.4)**. This abrupt decrease in Mo (ppm), but concurrent increase in %TOC and % Ca (unlike the T.W. George in **Figure 3.2**), make chemostratigraphic identification between Haynesville and the underlying Smackover lime formation perplexing in the Harvey core.

A cross-plot of Fe vs. detrital indicator titanium (Ti) of A) Goodrich Core, B) Harvey Core, C) Matthews Core, and D) Huffman Core is depicted in **Figure 3.5**. Iron and titanium exhibit an overall well-defined trend in the Bossier and a moderately linear trend in the Haynesville shale with some high Fe samples plotting to the right of the iron-titanium line. **Figure 3.6.A** is a crossplot of LECO-Sulfur vs. Fe, and **Figure 3.6.B** compares LECO-S against zinc, a redox sensitive productivity indicator.

Figure 3.7 depicts the affiliation of Ti with clay, by using Potassium (K) as a proxy for clay. Titanium makes a positive covariation with Potassium in both the Bossier and the Haynesville, just like Si and Ti made with Al in Figure 3. 2. **Figure 3.8** is a cross-plot of Fe vs. Al of A) T.W. George, B) Matthews, C) Frost, D) Harvey, E) Elm Grove, F) USA Double #1, and G) Carthage cores. Fe makes well defined linear trend with Ti in **Figure 3.5**, and with Al in **Figure 3.8**, indicating the association of iron in clay and its provenance to be detrital and terrestrial. Percent Total Inorganic Carbon (TIC) is plotted against percent concentration of Ca, Mg, Fe and Mn of the Carthage core (Panola County, TX) for carbonate tests in **Figure 3.9**. TIC is the sum of inorganic carbon in a specimen. TIC measurements were made on every foot of the 301 feet long Carthage core. TIC makes a well-defined trend with Ca in the Bossier-Haynesville shale,

and moderately-defined trend with Mg and Mn in the Haynesville shale, but lacks a robust relationship with Fe in either of the Bossier and the Haynesville shales. The Bossier also exhibits higher concentrations of Fe, Mg and Mn than the underlying Haynesville shale.

Figure 3.10 is clay, silica and carbonate ternary diagram using normalized calcium oxide (CaO), aluminum oxide (Al_2O_3), and silican dioxide (SiO_2). The Ca-Al-Si ternary is used to compare major shale components (Brumsack, 1989). Normalized weight percentages of SiO_2, 5 X Al_2O_3 and 2 X CaO are plotted to demonstrate the variation of quartz, clay and calcite in mudrocks respectively for A) T.W. George, B) Frost (from Texas) and C) Elm Grove, D) Matthews (from Louisiana). The Ca-Al-Si ternary depicts an overall similar composition of Haynesville shale as of the average grey shale, but Haynesville is dominated by carbonates. The decrease of clastics and clay-rich particles is concomitant with the rise in $CaCO_3$, evidential by the samples plotted along the calcite dilution line which shows the dilution of other elements (like Si and Al representing quartz and clay respectively) as calcite increases. The Ca-Al-Si ternary illustrates a slight enrichment of clay in the overlying Bossier formation, which is must be due to the decrease of carbonates in the Bossier compared to the underlying Haynesville.

3.2.2 Trace Metals and Depositional Environments

Figure 3.11 shows the comparison between the sulfur measured by the hand-held XRF and LECO-Sulfur of the Elm Grove core. Sulfur measurements are exaggerated by the hand-held XRF instrument; hence sulfur values generated from the handheld will not be utilized in this study. The chemostratigraphy of Enrichment Factors (EF) or the enrichment of anoxic indicators like Molybdenum (Mo), Vanadium (V), Uranium (U), and redox sensitive element Zinc (Zn) of three Haynesville cores (Huffman, Matthews and Harvey) are presented in **Figure 3.12**. Mo resident in the detrital phases of average shale is ~ 3ppm, which is typically only a small fraction of the Mo in the organic rich shale. Notice the EF_{Mo} increase at the lower Haynesville as we

move east in the ETB. Strong covariation between Mo and TOC suggest that organic matter is the primary host phase of Mo in the formation. The Fe-S-TOC ternary diagram (**figure 3.13**) is used to determine the amount of iron held in pyrite (Dean and Arthur, 1989). Almost all the Haynesville samples plot between the normal line and the pyrite line, and very few samples plot below the pyrite line in the ternary. **Figure 3.14** is a chemostratigraphy of the Elm Grove core comprising $EF_{Mo,}$ total organic carbon (TOC), Degree of pyritization (DOP_T), V/Cr values and Si. A positive correlation can be observed between EF_{MO}, TOC, and DOP_T. A moderately defined relationship between LECO-S and TOC of the Elm Grove core is demonstrated in **Figure 3.15**. **Figure 3.16** displays cross-plots of Mo against TOC of cores across the East Texas Basin, and the variation of Mo concentration in the Haynesville across the ETB is depicted in **Figure 3.17**.

The variation of productivity indicator P and it's relation to TOC and C/N is depicted in the chemostratigraphy of the T.W. George core in **Figure 3.18**. **Figures 3.19** and **3.20** shows $\delta^{13}C$ vs. C/N ratio and $\delta^{13}C$ vs. $\delta^{15}N$ respectively. These plots are used for determining organic matter provenance purpose.

3.2.3 Enrichment Factors (EF)

Enrichment factor (EF) is defined as any deviation from the chemical composition of average shale (average shale values after Wedepohl, 1971, 1991). Enrichment or depletion can be seen in an enrichment factor ratio, calculated by

$$EF = (\text{element in ppm/Al in ppm})_{\text{sample}} \,/\, (\text{element in ppm/Al in ppm})_{\text{standard}}$$

If EF > 1, then the element is enriched relative to average shale, and if EF <1, the element is depleted compared to average shale.

3.2.4 Degree of Pyritization (DOP)

Degree of pyritization (DOP) provides insights on the redox condition during deposition (Raiswell et al, 1988). Degree of pyritization is the ratio of pyritic iron over total reactive iron, but assuming all Fe is reactive Fe, DOP_T can be approximated as:

$DOP_T = Fe_{pyr} / Fe_{tot}$ (Raiswell and Berner, 1986).

Value cut offs for degree of pyritization as defined by Raiswell and Berner (1986) are as follows,

$DOP_T < .42$ = oxic,

DOP_T from .46 to .80 = dysoxic, and

DOP_T from .55 to .93 as anoxic (Raiswell and Berner, 1986, Raiswell et al, 1988).

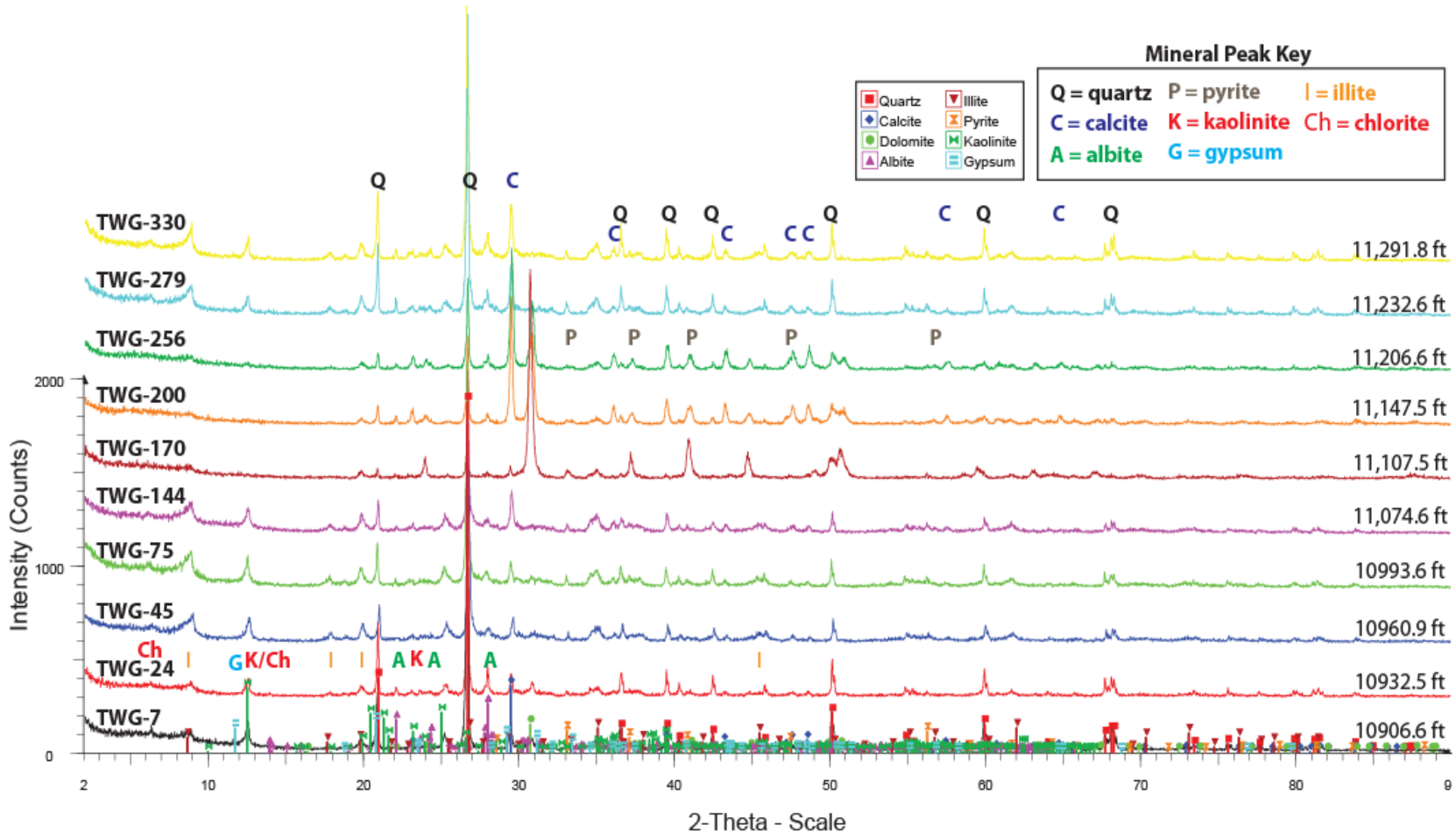

Figure 3.1 XRD analysis of the T.W. George Core. Bossier Samples include the bottom five samples (7, 24, 45, 75 and 144) and the top six are Haynesville. Sample depths (in feet) are shown above each spectrum, on right.

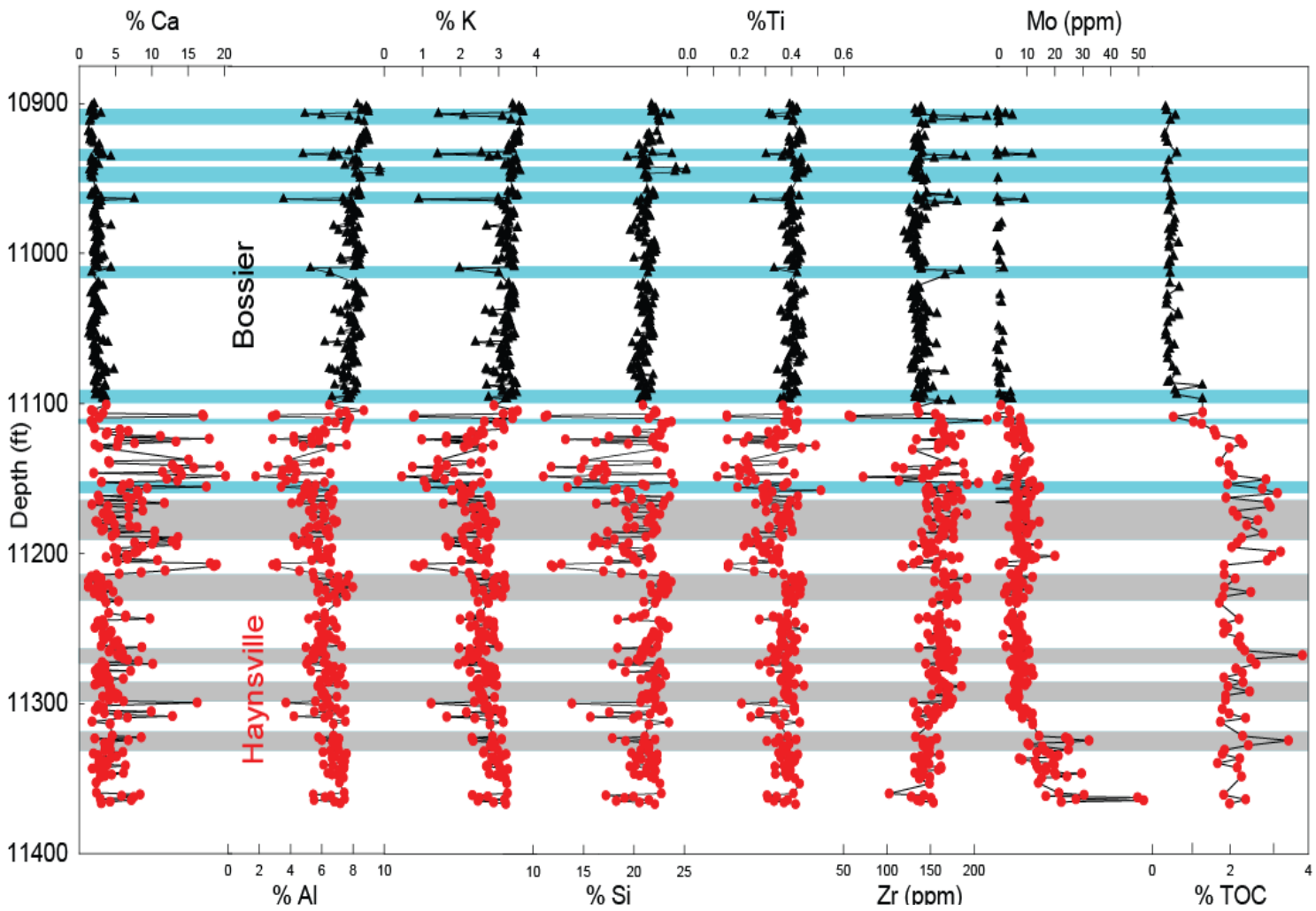

Figure 3.2 Chemostratigraphy of the T.W. George (Harrison County) with the Bossier-Haynesville contact. Percent Ca, % Al. % K, % Si, % Ti, Zr (ppm), Mo (ppm) and %TOC are plotted. Possible detrital silica has been highlighted in cyan and biogenic silica has been highlighted in grey after close observation of detrital proxies like wt. percent silica, titanium, zirconium and productivity proxy total organic carbon (TOC).

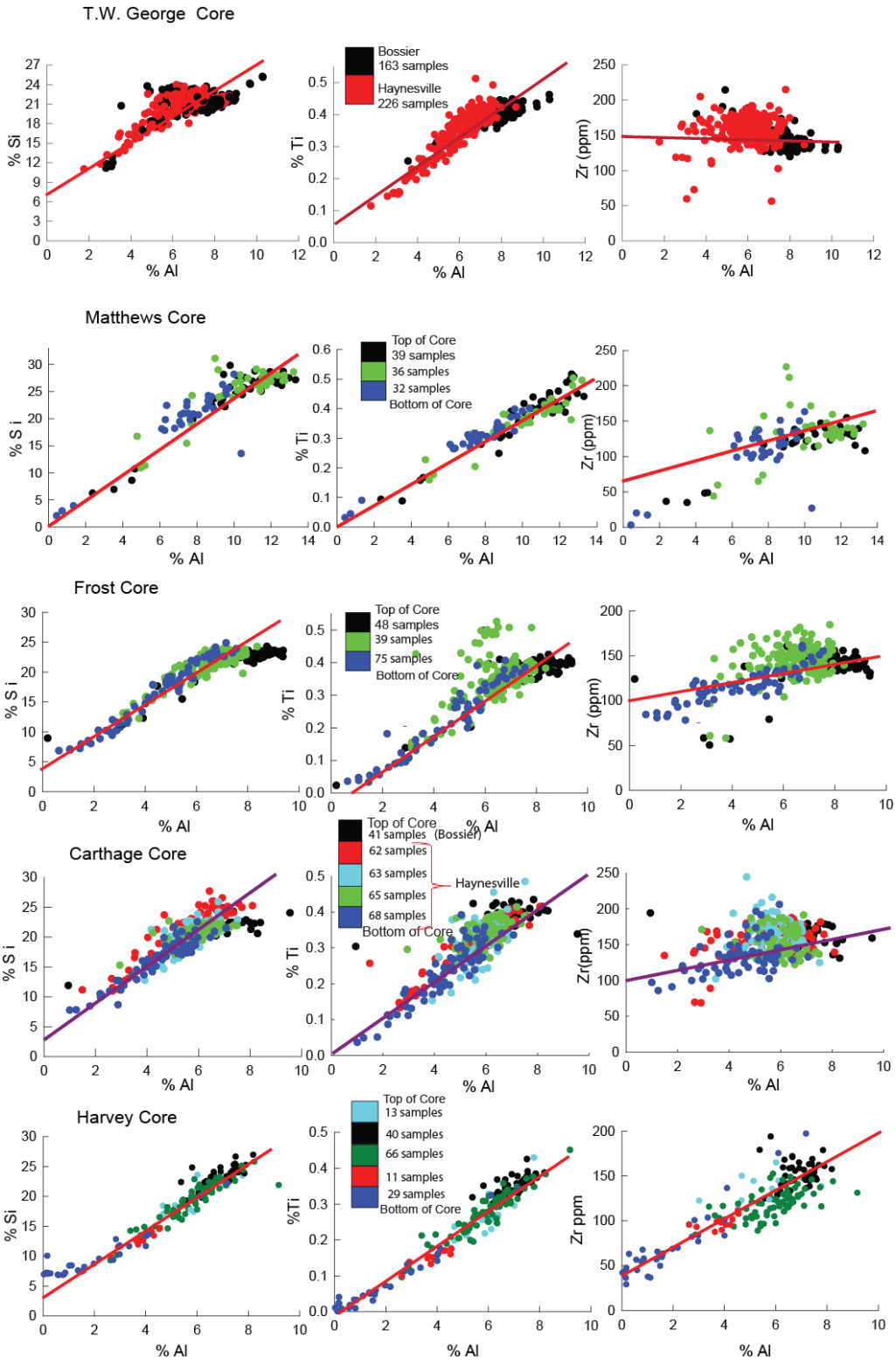

Figure 3.3 Cross-plots of detrital elements like Si, Ti and Zr vs. Al from the ETB. The red lines are drawn to represent the best fit trend.

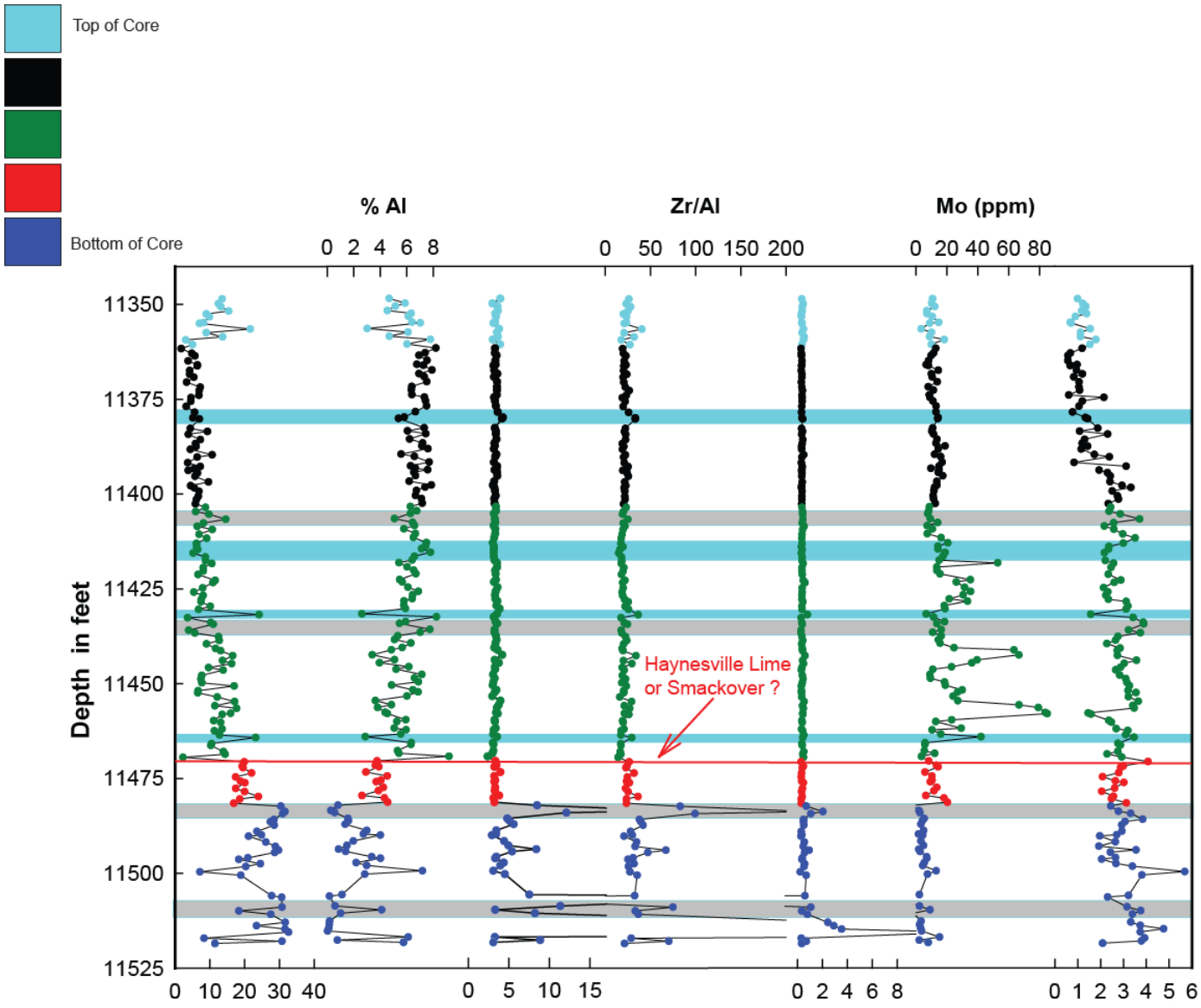

Figure 3.4 Chemostratigraphy of elements normalized to clay (Al) for the Harvey core. Possible detrital silica has been highlighted in cyan and biogenic silica has been highlighted in grey after observation of detrital proxies.

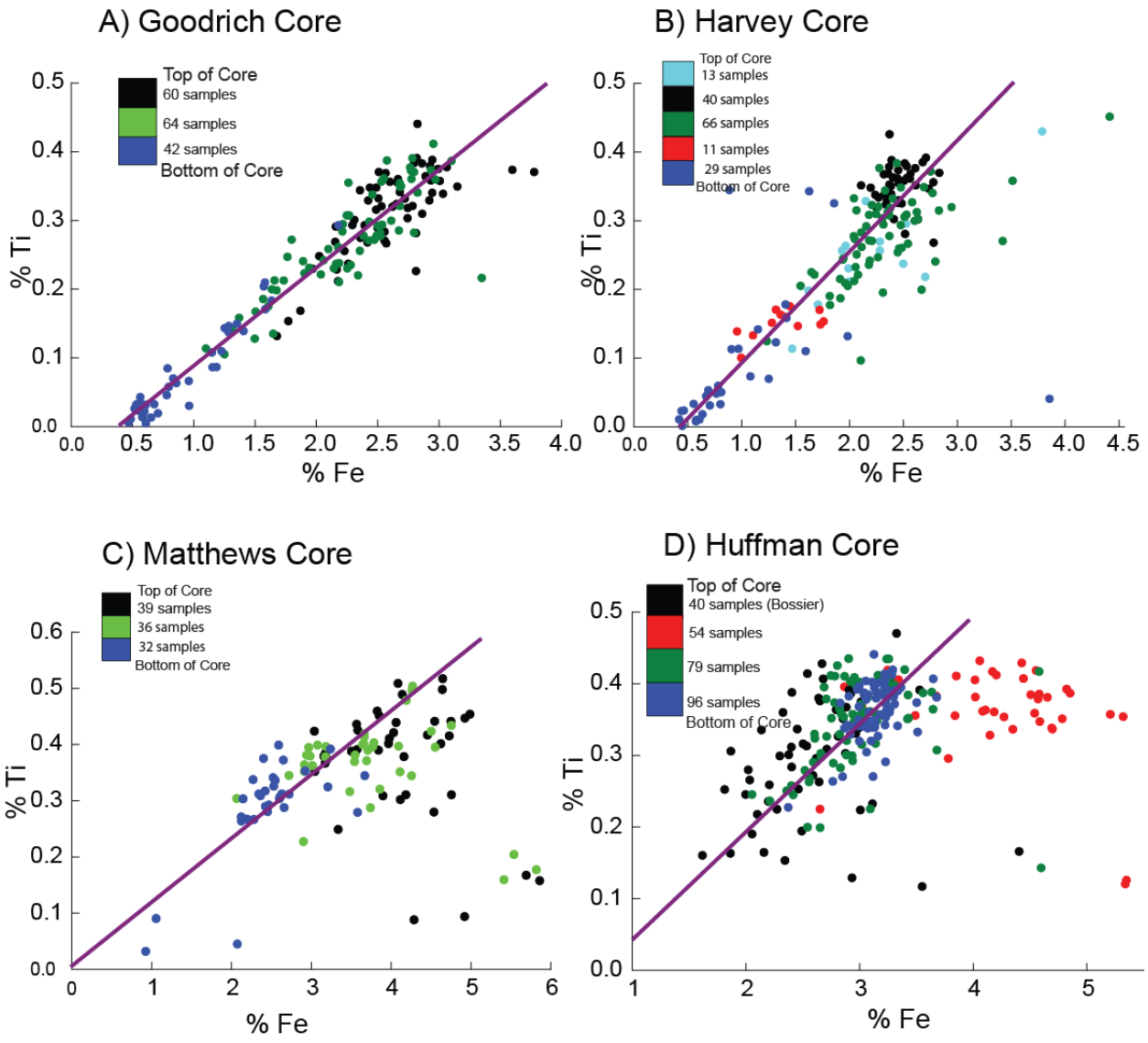

Figure 3.5 Crossplots of detrital proxy Ti vs. Fe of A) Goodrich, B) Harvey, C) Matthews, and D) Huffman cores. The purple lines are drawn to represent the best fit trend.

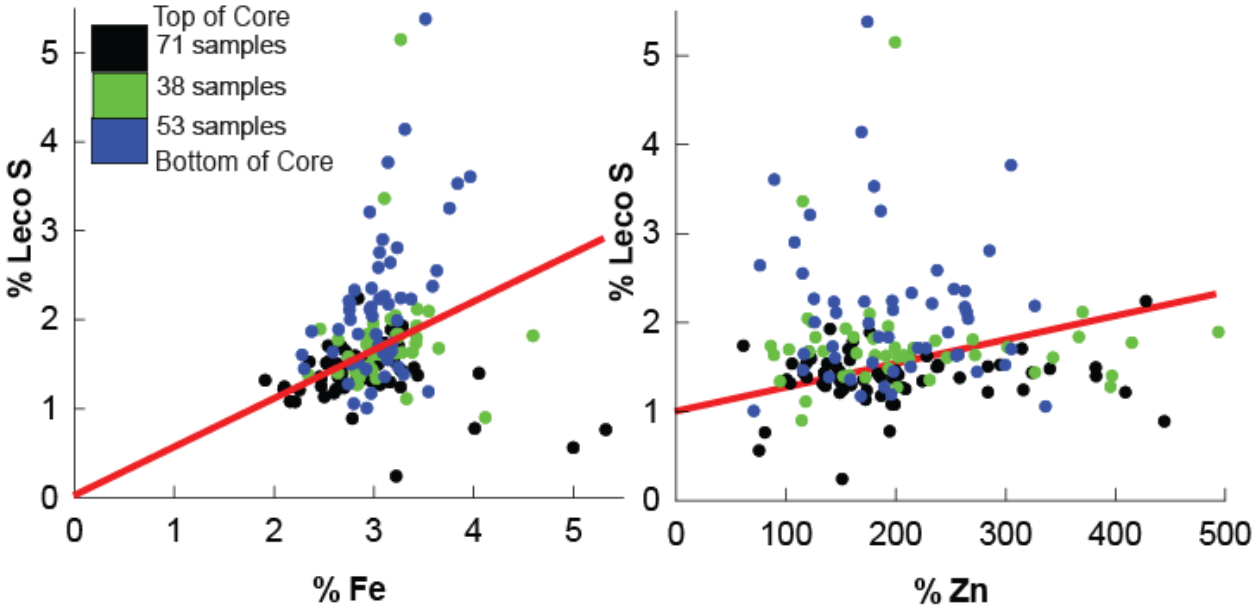

Figure 3.6 Crossplots of A) percent Fe vs. S, and B) percent Zn vs. S of the Elm Grove core. The red lines are drawn to represent the best fit trend.

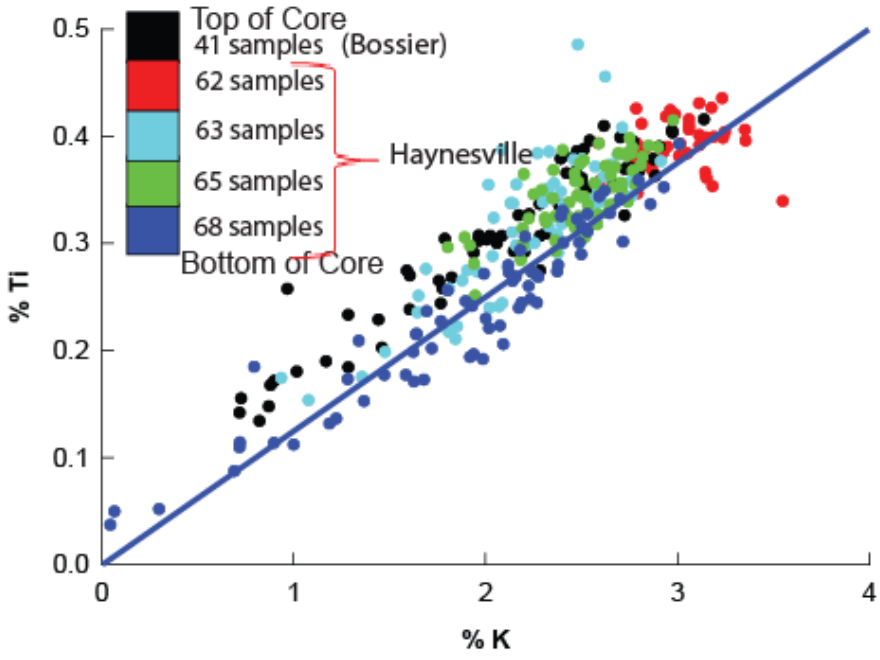

Figure 3.7 Crossplot of Ti vs. K indicates titanium's affiliation with clay in the Carthage core. The black samples represent the Bossier shale. The blue line is drawn to represent the best fit trend.

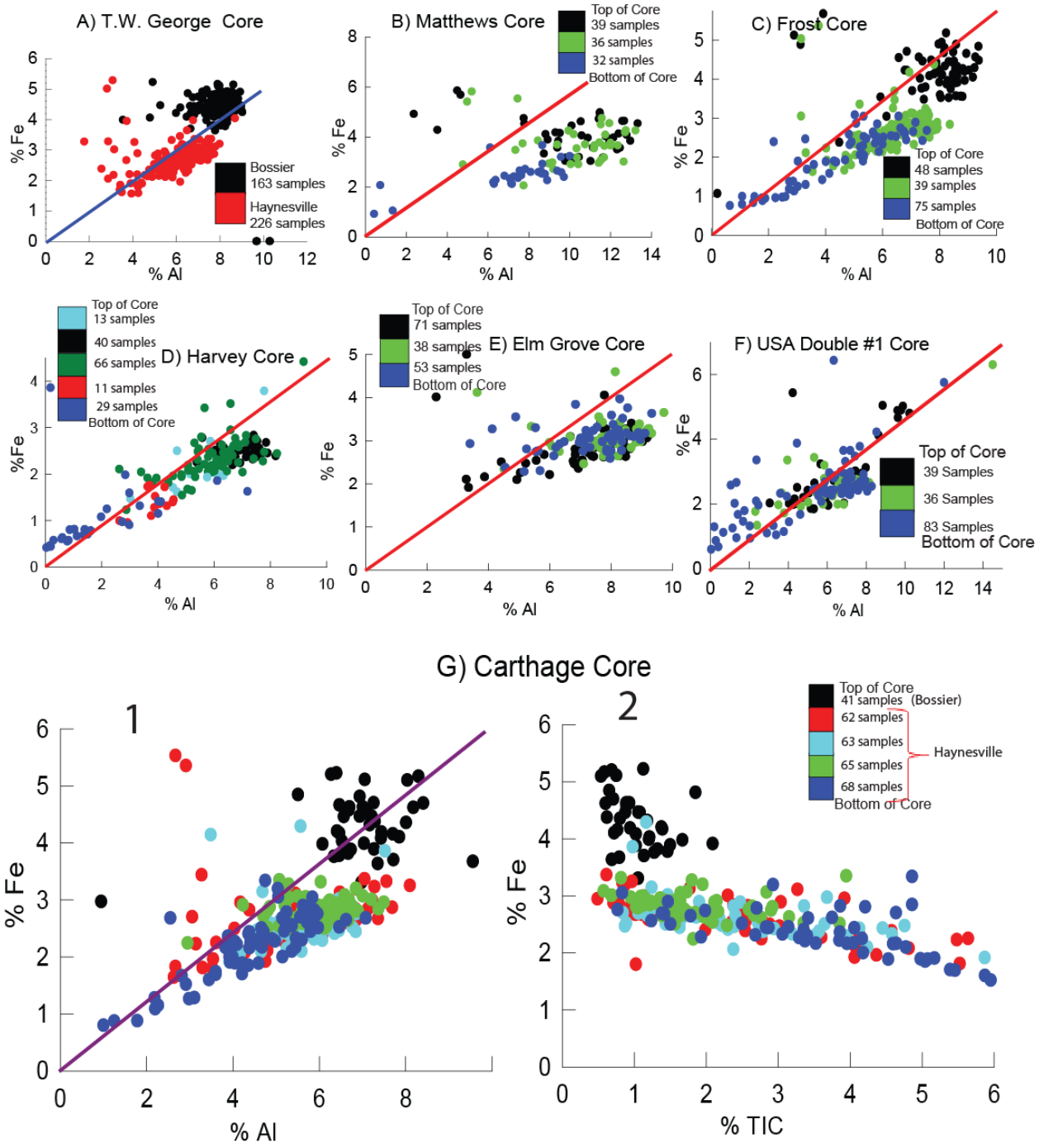

Figure 3.8 Crossplots of Iron against Aluminum of A) T.W. George, B) Matthews, C) Frost, D) Harvey, E) Elm Grove, F) USA Double #1, and G1) Carthage cores. Fe vs. TIC is plotted in Figure G2) Carthage core. The blue, red and purple lines are drawn to represent the best fit trend.

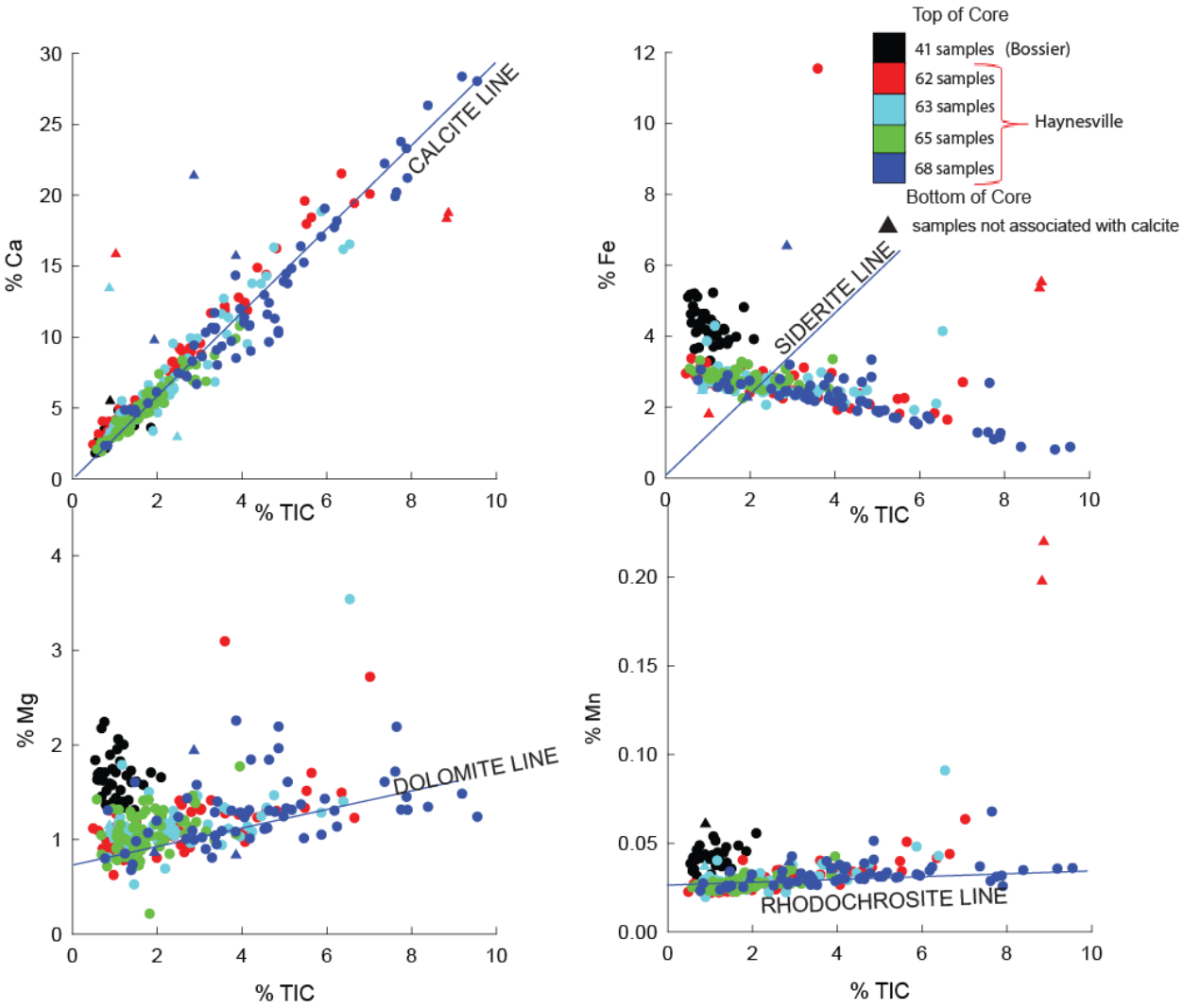

Fig 3.9 Total organic Carbon (TIC) is plotted against elements Ca, Fe, Mg, and Mn of the Carthage Core. The blue lines are drawn to represent the best-fit line. Notice the righteous calcite line, and the lack of a siderite trend.

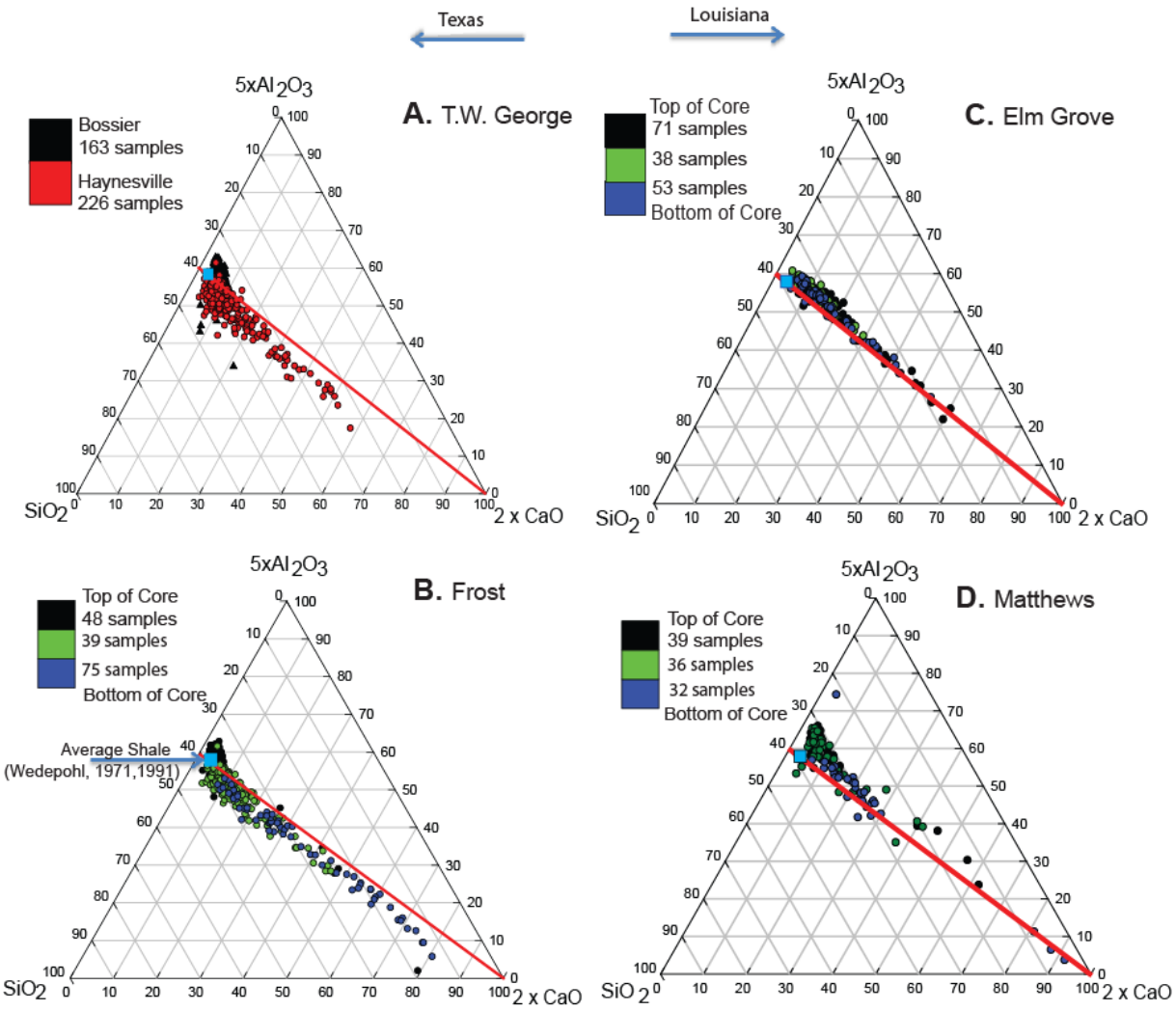

Figure 3.10 Ca-Al-Si relationship of the western cores (T.W. George and Frost), and the eastern cores (Elm Grove and Matthews) in the East Texas Basin, after Brumsack (1989). The square denotes the average gray shale (Wedepohl, 1971, 1991), and the red line represents the calcite dilution line.

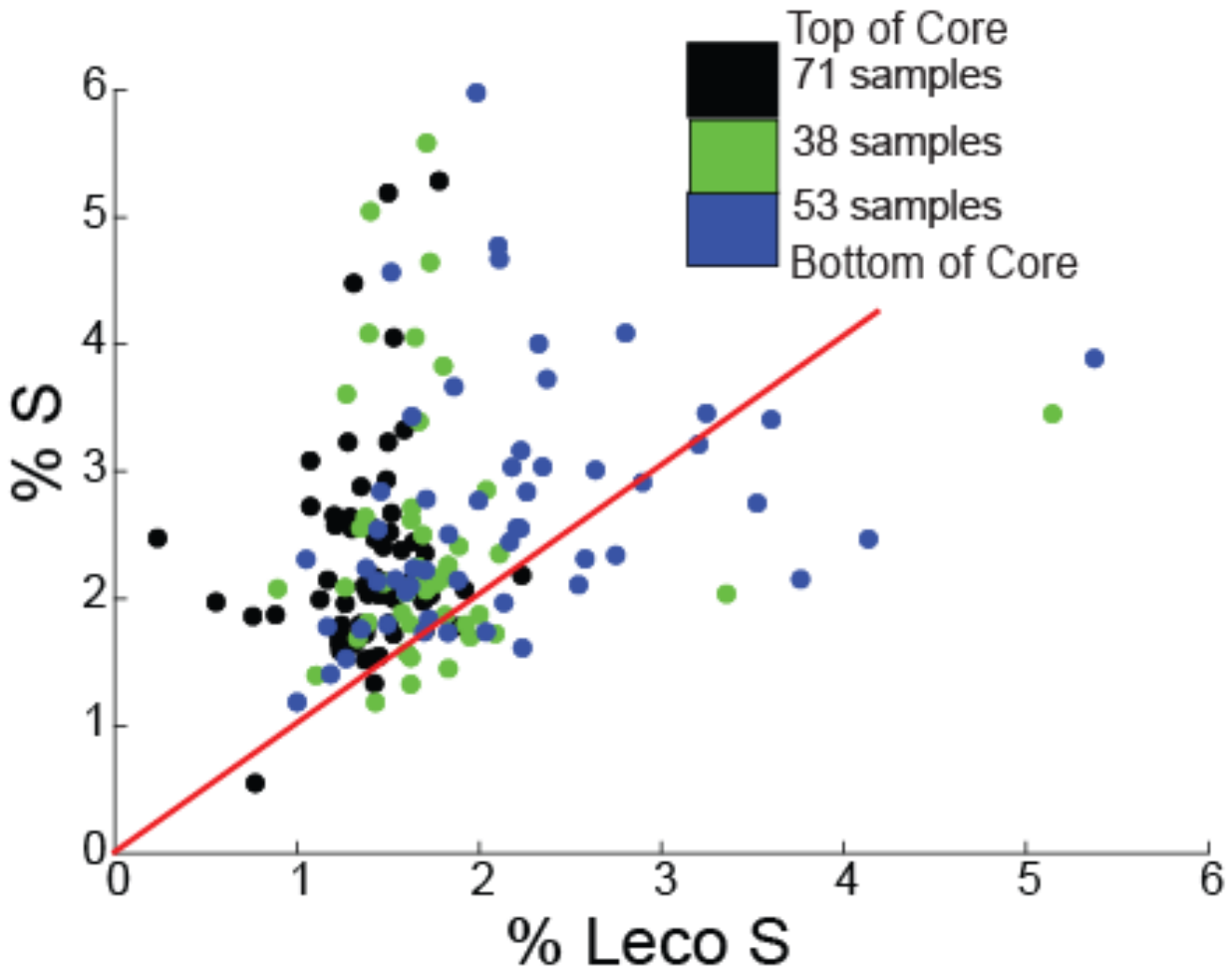

Figure 3.11 LECO S vs. XRF measured S from Elm Grove core. The red line is drawn to represent the best fit trend.

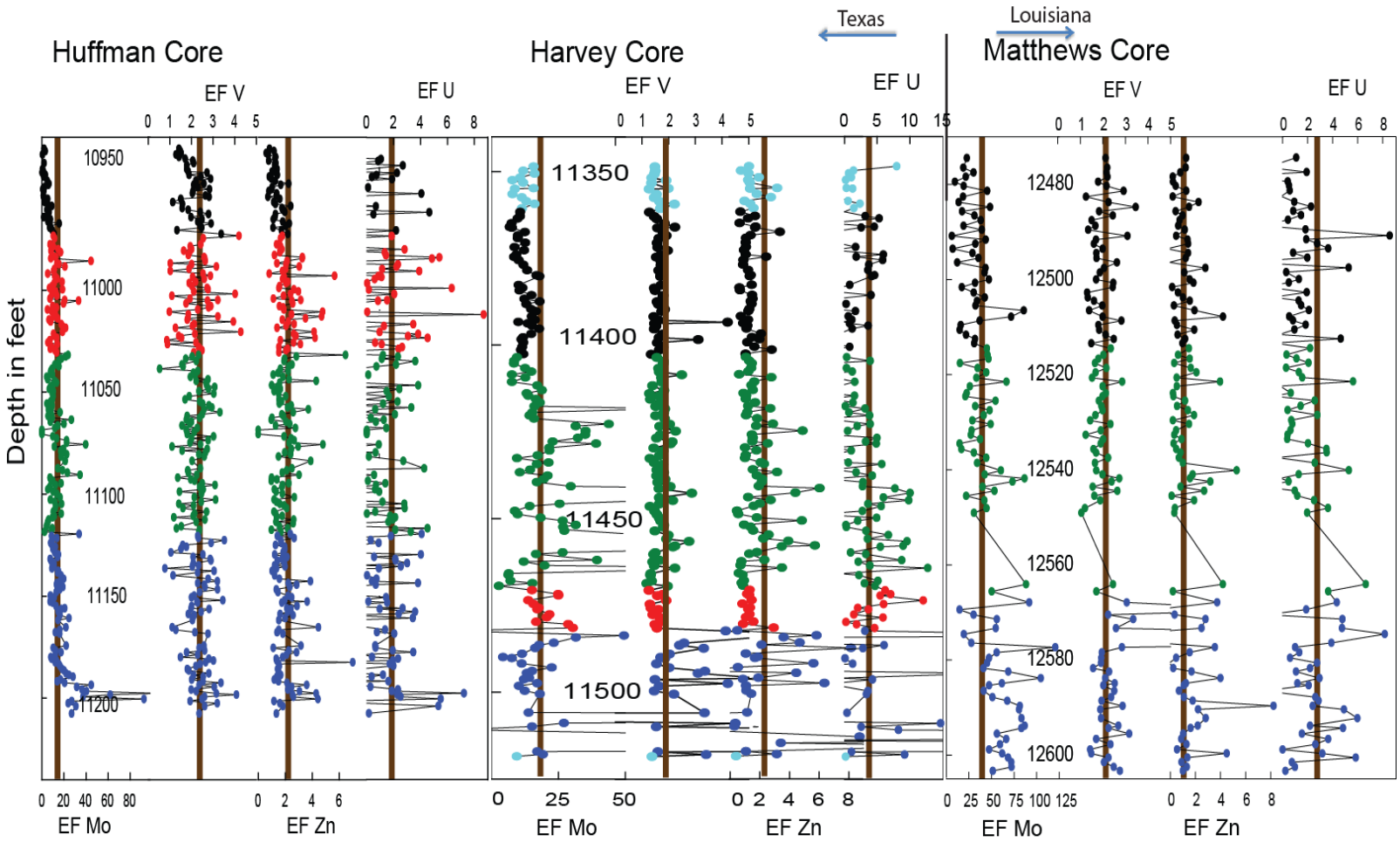

Figure 3.12 Chemostratigraphy of the enrichment factor (EF) of the redox, sensitive elements (Mo, V, Zn and U) of Huffman, Harvey and Matthews cores. Vertical brown lines represent an average EF value.

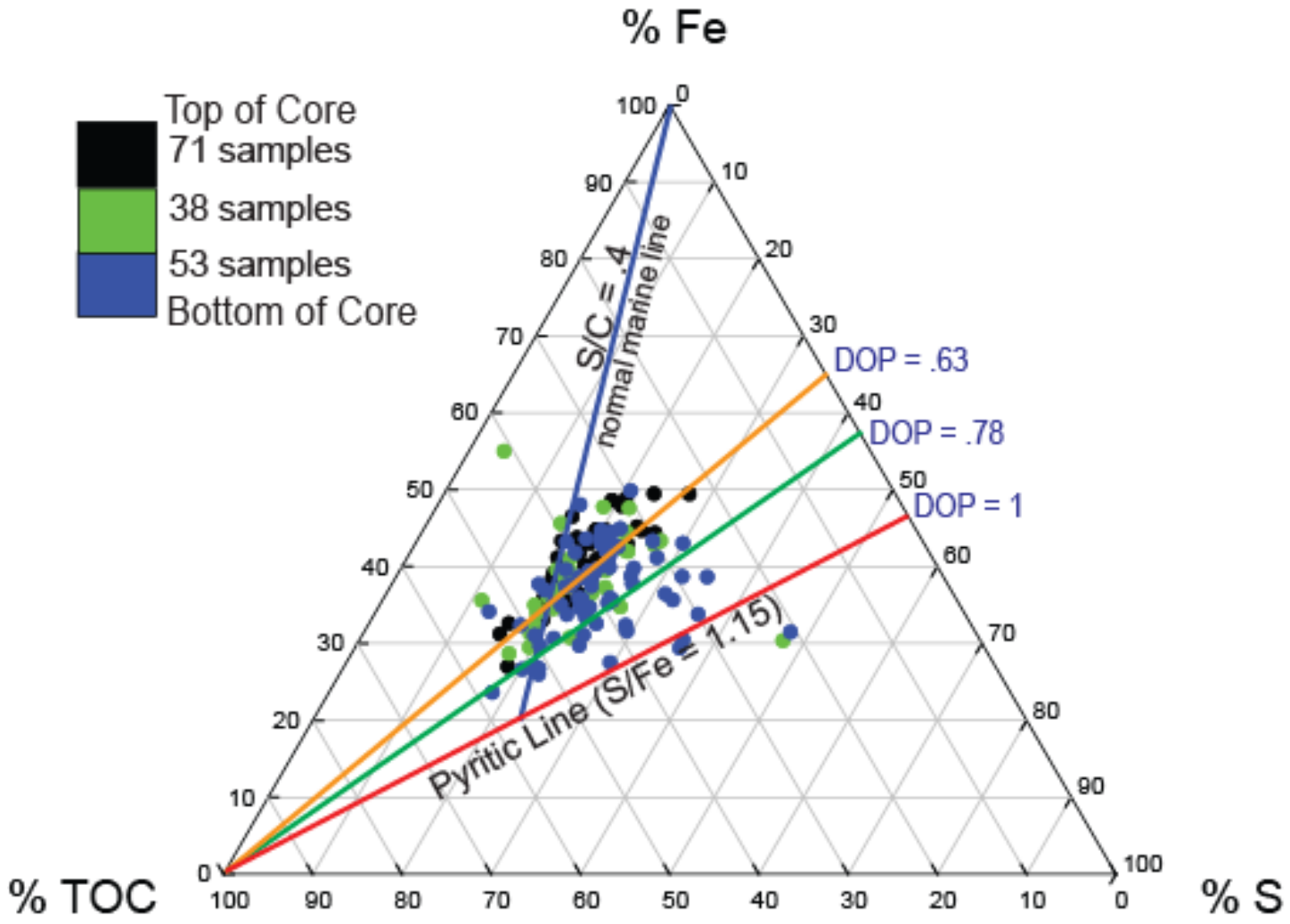

Figure 3.13 Fe-S-TOC ternary diagram of the Elm Grove core (after Dean and Arthur, 1989).

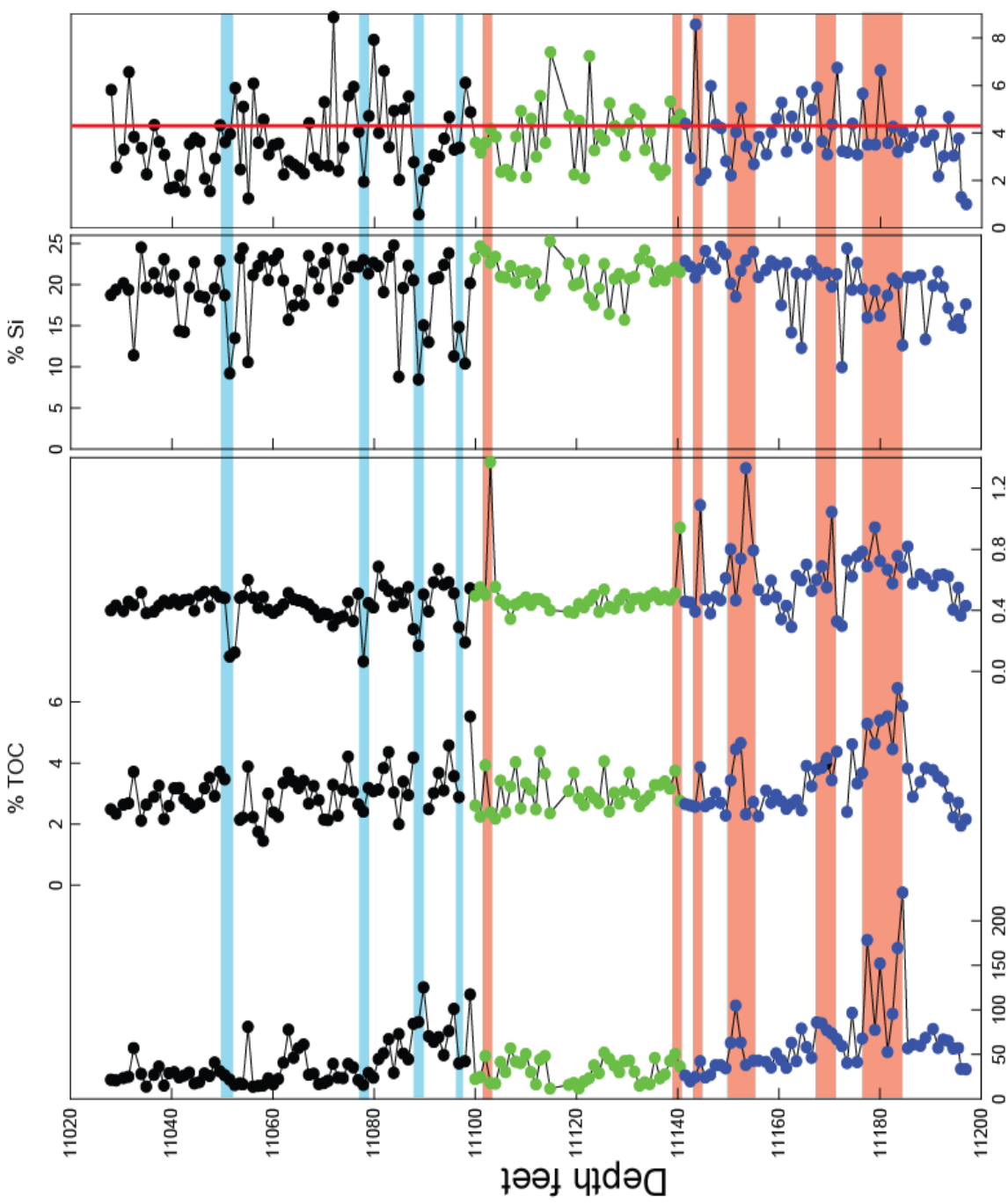

Figure 3.14 Chemostratigraphy of Elm Grove core depicting relationship between anoxia proxies (Mo, V/Cr, TOC and DOP_T) and concentration of Si (representing Silica sedimentation).

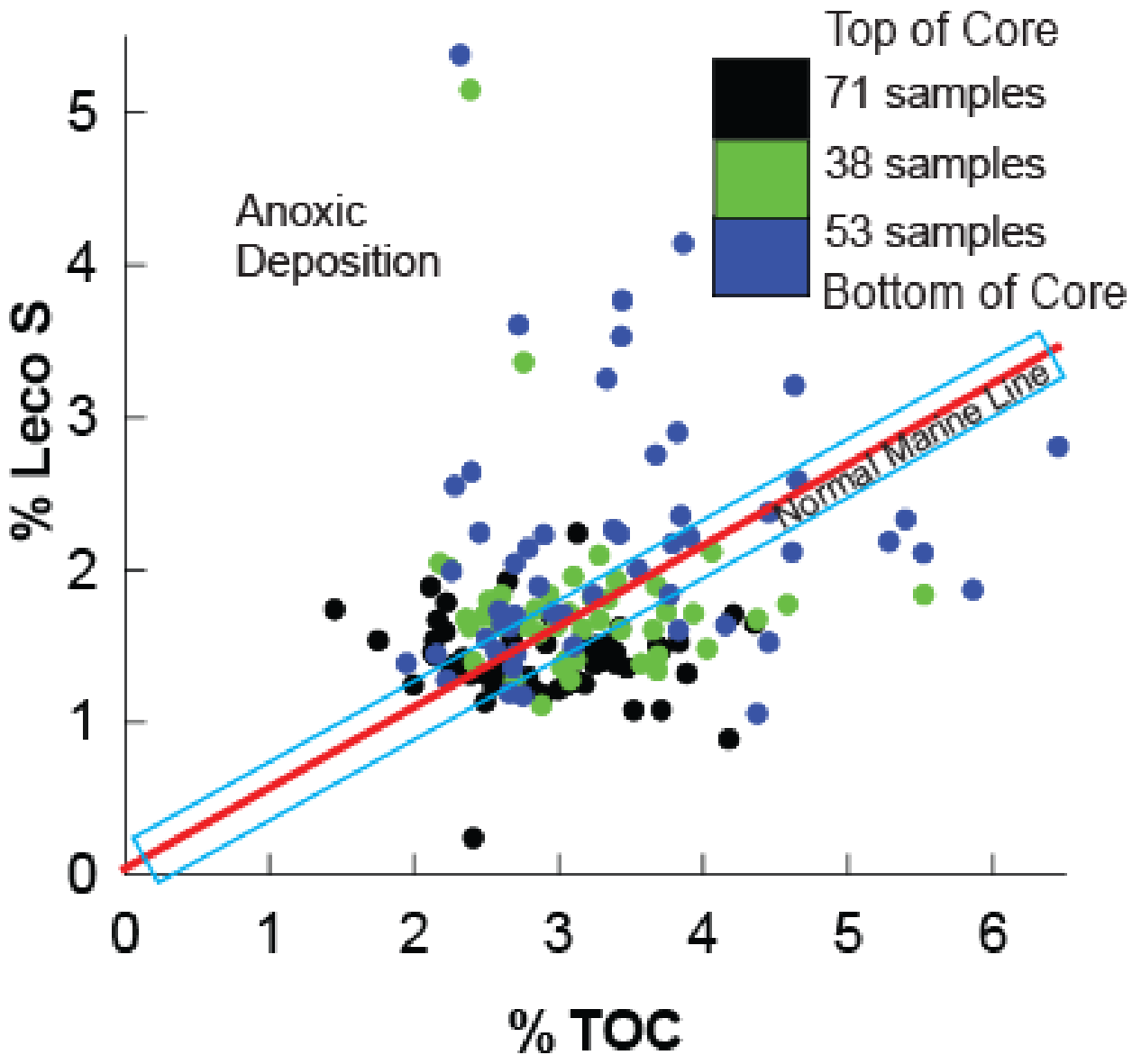

Figure 3.15 Crossplot of LECO Sulfur vs. (TOC) in the Elm Grove core. The red line represents normal marine conditions, and the blue rectangle represents an acceptable range of “normal marine” conditions (Berner and Raiswell, 1983).

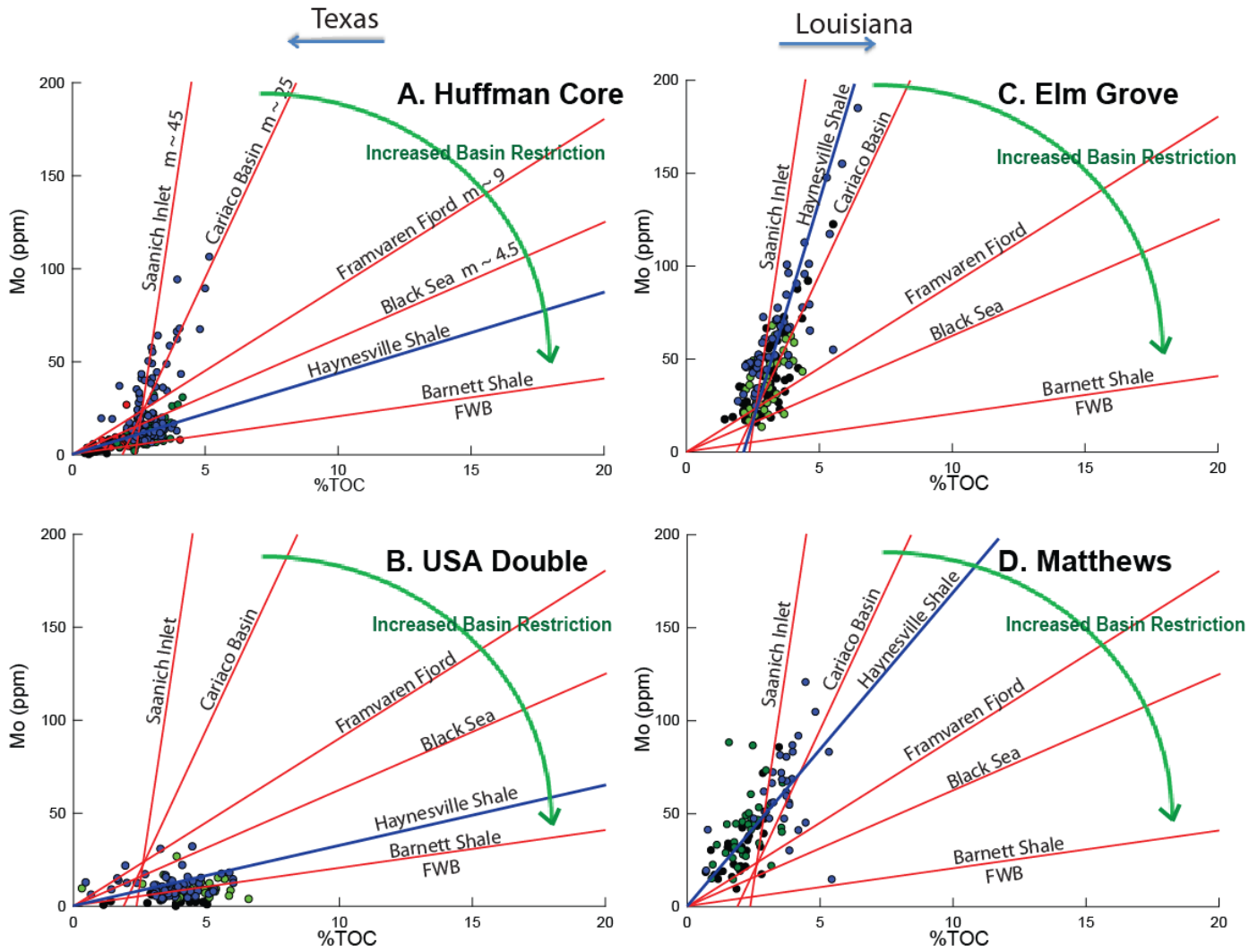

Figure 3.16 Mo VS TOC biplots of four Bossier-Haynesville cores spread around the East Texas Basin. The red line denotes the best fit Mo-TOC relationship of the four modern anoxic basins, and the blue line is the trend made by the Haynesville samples of ETB. (after Algeo and Lyons (2006) and Rowe et al., (2008).

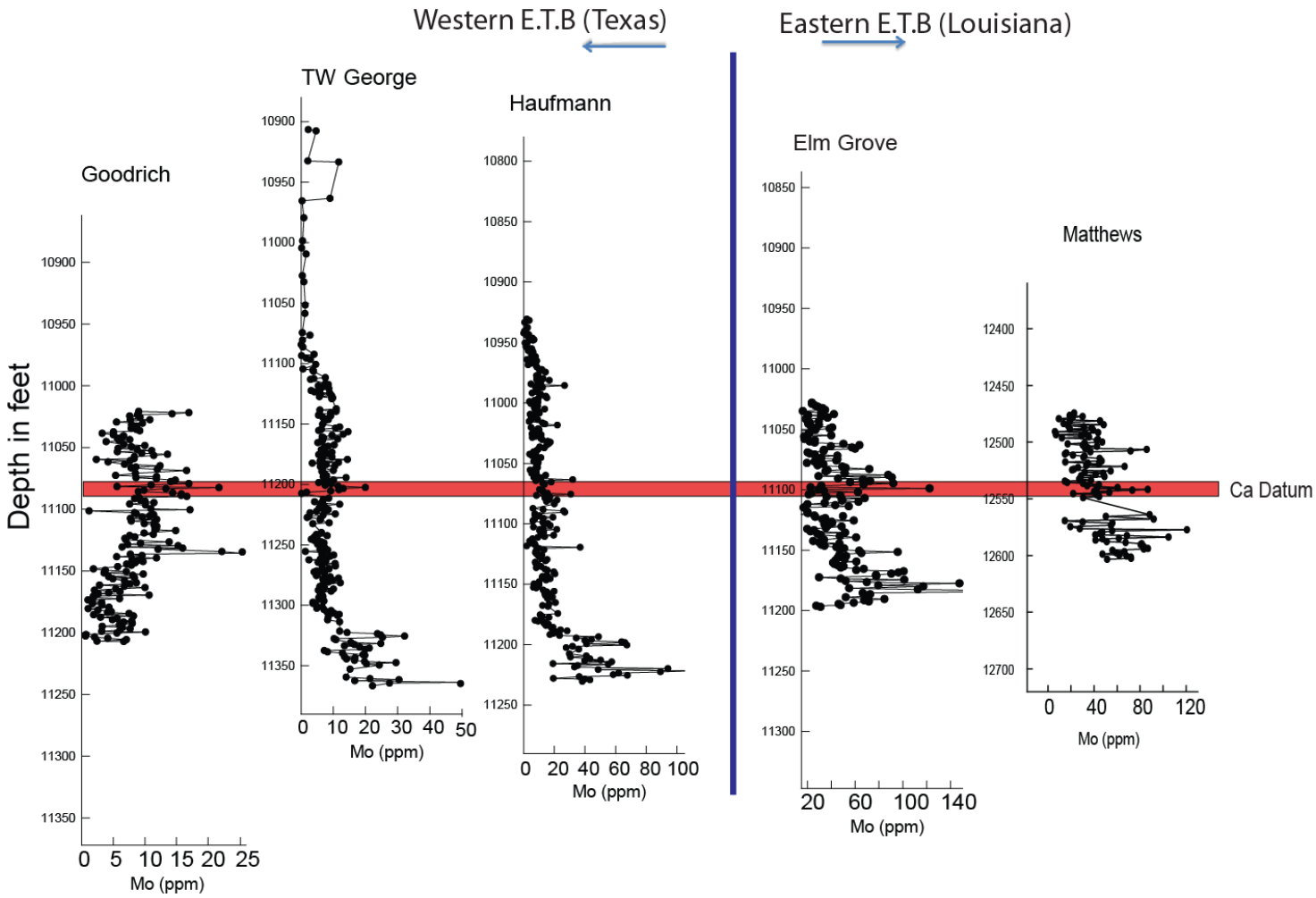

Figure 3.17 Variation in Mo concentration across the East Texas Basin. Ca chemostratigraphy not shown (refer to Figure 4.5 for Ca chemostratigraphy).

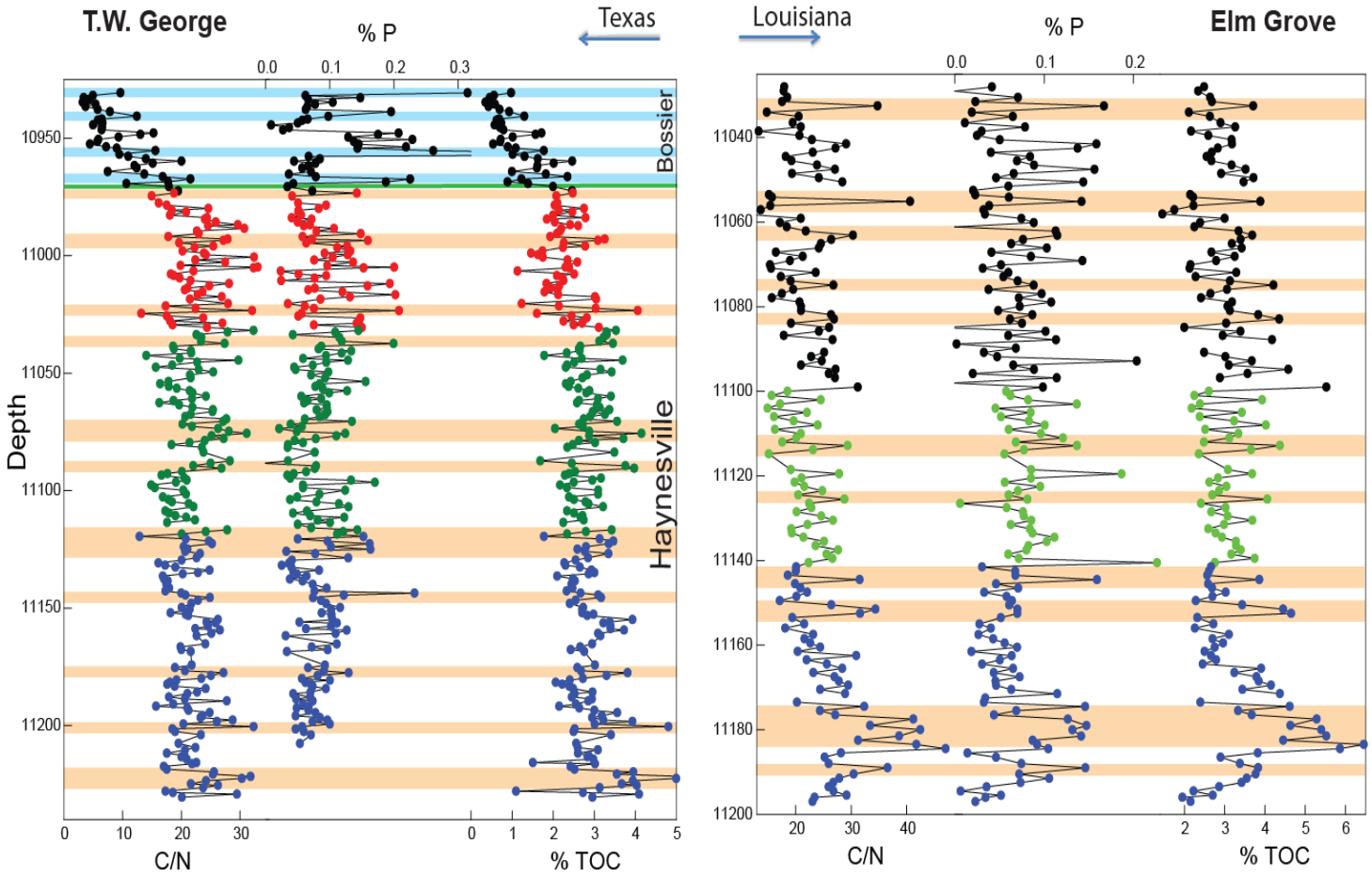

Figure 3.18 Chemostratigraphy of C/N, %P and TOC of the TW. George and the Elm Grove Core. Highlighted in blue is high productivity zones (indicated by high P content), but relatively low accumulation of organic carbon probably due to the more oxygenated waters during Bossier deposition. Highlighted in red high %P and high %TOC, attributed anoxic-euxinic.

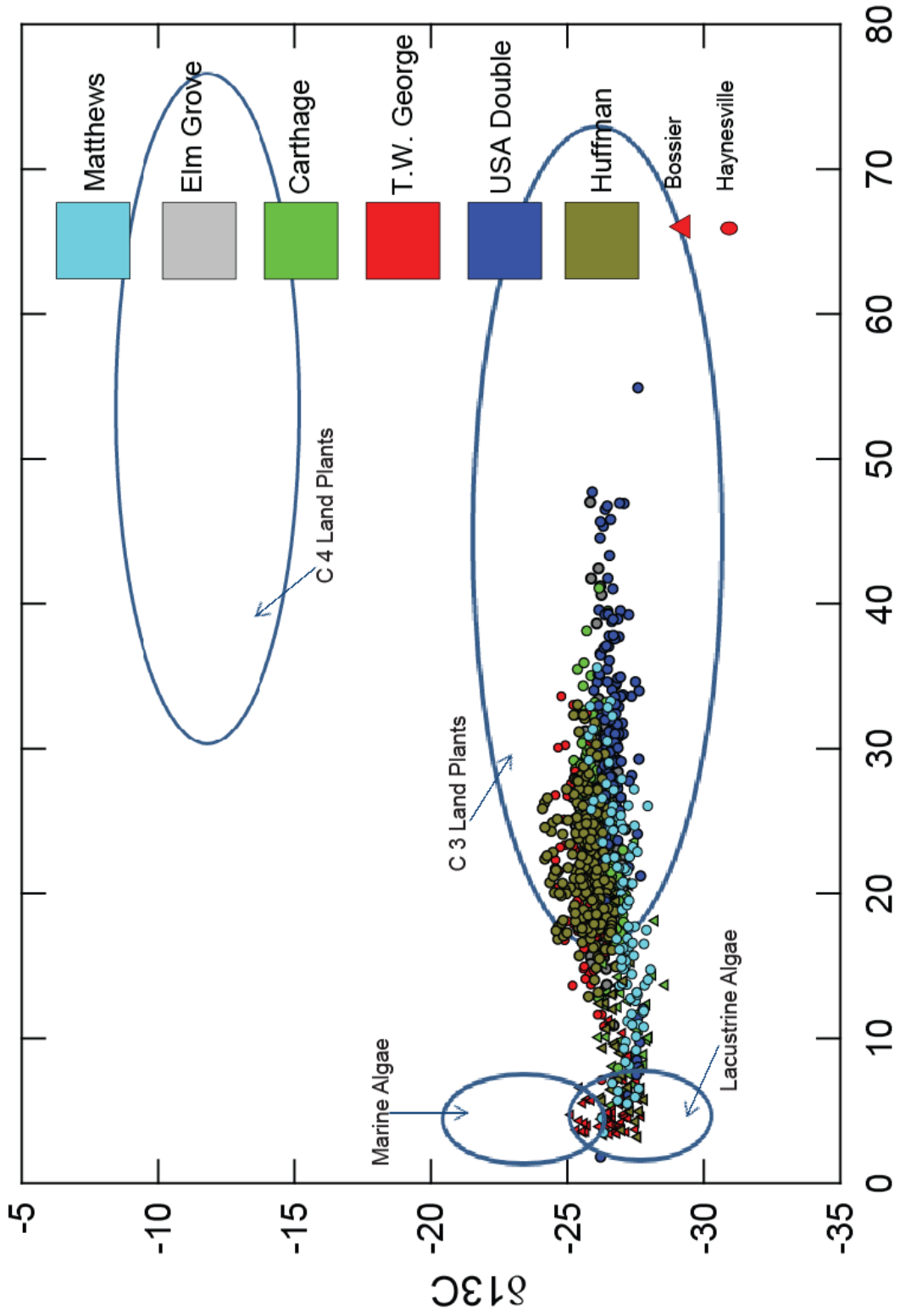

Figure 3.19 Identifier of the provenance of organic matter in the sediments using $\delta^{13}C$ and C/N ratio (from Meyers, 1997).

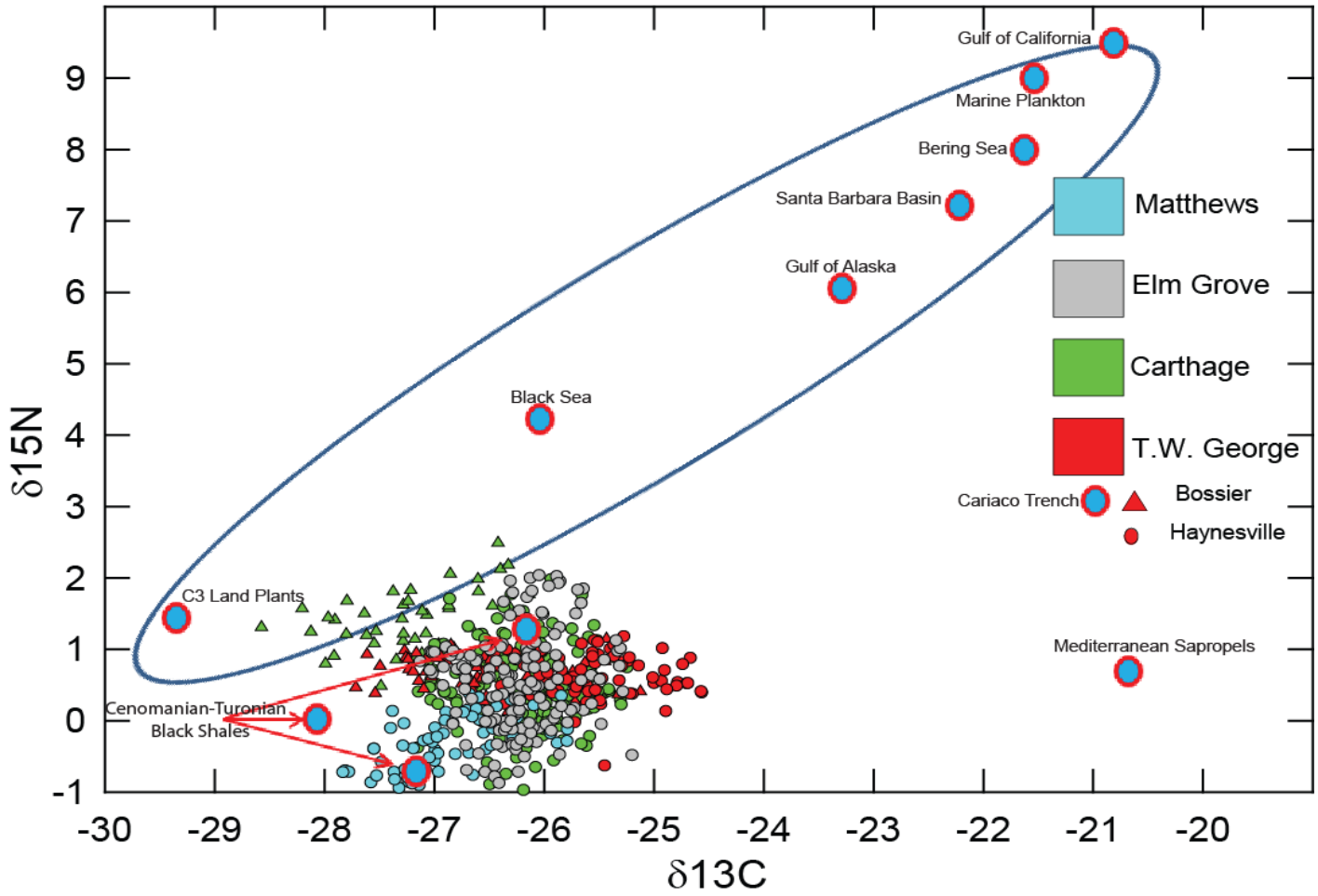

Figure 3.20 Organic matter source using $\delta^{13}C$ and $\delta^{15}N$. (From Meyers, 1997; originally noted by Peters et al (1978). Data used by Meyers (1997) from – Pride et al., unpublished data; Peterson and Howarth, 1987 Meyers et al, 1986; Rau et al., 1987; Calvert et al.,1992; Fontugne and Calvert, 1992).

3.3 Tables

Table 3.1 shows the average values from the isotope analyses on the Bossier and the Haynesville cores used for interpretation. Cumulative average is the calculated average of the averages from different cores. This cumulative average is used as an overall average of the Bossier or the Haynesville formation from East Texas Basin in this study. **Tables 3.2** and **3.3** show the average from different cores, and the cumulative average of the major and trace elements concentrations respectively. Major and trace elemental data was collected using a hand-held X-ray fluorescence instrument also described in chapter two (Methods).

Table 3.1 Average values of total organic carbon(TOC), nitrogen(N), ratio of C/N, total inorganic carbon (TIC), and different isotope analysis ($\delta^{13}C$ and $\delta^{15}N$) on the Bossier and the Haynesville cores used for interpretation.

Bossier						
	TOC	% N	C/N	$\delta^{15}N$	$\delta^{13}C$	TIC
TW. George	0.49	0.112	5.242	0.619	-26.594	-
Carthage	0.13	1.205	11.387	1.444	-27.230	1.039
Huffman	1.11	0.135	9.808	-	-26.890	-
Cumulative AVG	0.57	0.484	8.813	1.032	-26.905	1.039
Haynesville						
	TOC	% N	C/N	$\delta^{15}N$	$\delta^{13}C$	TIC
Frost						
Goodrich						-
TW. George	2.21	0.130	20.537	0.485	-25.917	-
USA Double	3.75	0.145	30.529	-	-26.509	-
Harvey	-	-	-	-	-	-
Carthage	2.86	0.128	25.888	0.303	-26.181	2.780
Huffman	2.93	0.156	21.801	-	-25.473	-
Elm Grove	3.15	0.155	23.519	0.479	-26.231	-
Matthews	2.61	0.171	18.784	-0.658	-27.316	-
Cumulative AVG	2.92	0.148	23.509	0.152	-26.271	2.780

Table 3.2 Average major elemental weight percent of the different Bossier and Haynesville cores analyzed used for interpretation in the study. Average Leco Sulfur value is the average value from the 164 Elm Grove samples analyzed for Sulfur.

Bossier												
	%Mg	%Al	%Si	%P	%S	%K	%Ca	%Ti	%Mn	%Fe	V (ppm)	Cr (ppm)
T.W. George	1.553351	7.91788	21.31908	0.146	0.62304	3.184002	2.378669	0.404	0.0455	4.38633	128	51
Carthage	1.596237	6.95157	21.89189	0.252	1.6843	2.983788	3.233258	0.388	0.0422	4.29822	152	82
Huffman	1.414367	7.53677	20.05373	0.123	2.79911	2.892971	5.303386	0.358	0.0447	4.27213	181	52
Cumulative AVG	1.574794	7.43473	21.60548	0.199	1.15367	3.083895	2.805964	0.396	0.0438	4.34227	153	61
Haynesville												
	%Mg	%Al	%Si	%P	%S	%K	%Ca	%Ti	%Mn	%Fe	V (ppm)	Cr (ppm)
Frost	1.298316	6.32974	20.30094	0.104	1.1698	2.339159	7.479488	0.360	0.0331	2.91385	119	85
Goodrich	1.326327	4.85912	17.15875	0.083	1.13796	1.744191	13.53249	0.236	0.0293	2.04652	86	68
TW. George	0.944477	6.02754	20.5138	0.113	0.72533	2.476558	5.816091	0.350	0.0273	2.73718	107	54
USA Double	1.1402	5.7137	19.6944	0.119	1.27712	2.030457	12.23938	0.271	0.0379	2.60702	103	86
Harvey	1.213344	5.26347	18.1422	0.081	0.87632	1.880188	12.67712	0.249	0.0295	2.04475	95	84
Carthage	1.198805	5.40041	19.54271	0.165	1.88555	2.182683	8.420399	0.299	0.0313	2.65436	111	84
Huffman	1.026562	6.43293	19.31746	0.092	3.2108	2.390284	7.638988	0.342	0.0258	3.17889	201	67
Elm Grove	0.857933	7.37105	20.00687	0.072	2.46095	2.700102	8.226894	0.345	0.0216	3.02105	267	76
Matthews	1.834952	9.31488	23.16471	0.119	3.07352	2.962186	7.823461	0.347	0.0278	3.60524	279	79
Cumulative AVG	1.204546	6.30143	19.7602	0.10526	1.75748	2.300645	9.317146	0.31105	0.0293	2.75654	273.584	97.5213
				Leco S =	1.7432	Elm Grove						

Table 3.3 Average major elemental weight percent of the different Bossier and Haynesville cores analyzed and used for interpretation in the study.

Bossier										
	Co (ppm)	Ni (ppm)	Cu (ppm)	Zn (ppm)	Th (ppm)	Rb (ppm)	U (ppm)	Sr (ppm)	Zr (ppm)	Mo (ppm)
T.W. George	11	40	36	77	13	147	1	193	139	-3
Carthage	10	41	37	86	14	147	-9	471	164	-1
Huffman	-	35	72	103	11	150	-2	281	119	3
Cumulative AVG	10	39	48	89	13	148	-3	315	141	0
Haynesville										
	Co (ppm)	Ni (ppm)	Cu (ppm)	Zn (ppm)	Th (ppm)	Rb (ppm)	U (ppm)	Sr (ppm)	Zr (ppm)	Mo (ppm)
Frost	9	51	38	16	11	132	0	314	138	7
Goodrich	7	59	36	65	10	116	1	443	141	8
TW. George	9	54	34	99	12	138	4	274	157	9
USA Double	-	-	-	-	-	-	-	-	-	-
Harvey	7	61	36	90	9	123	4	282	119	15
Carthage	9	60	36	91	11	134	0	465	152	10
Huffman		60	73	142	11	141	2	314	129	17
Elm Grove	105	92	105	234	10	136	5	275	124	47
Matthews	-	-4	-8	131	11	131	6	218	121	43
Cumulative AVG	21	62	50	124	12	150	3	369	216	20

CHAPTER 4

DISCUSSION

The discussion though primarily focused on the Bossier-Haynesville shale of the East Texas Basin, will present and compare results from other shale formations to expand our knowledge of black shales, and to better understand the Bossier-Haynesville formation. To serve this purpose detrital elements (Al, Ti, Zr), carbonates (Ca, Mg, Mn, Sr) and organic associations (Mo, Zn, Ni, Cu, Cr, V) (Vine and Tourtelot, 1970, Brumsack, et. al, 2003), along with total inorganic carbon (TIC), total organic carbon (TOC), δN^{15} and δC^{13} isotopes, C/N ratio, other major and trace elements generated from X-ray fluorescence and their ratios are evaluated in the context of. The bulk geochemistry of the Haynesville can be used to identify changes in the mineralogy of the shale formation. Crossplots of major elements versus Al are used to identify the elements presence in clay. Calcium mineral phases can be identified by cross-plots TIC versus calcium. TOC-S-Fe ternary along with concentrations of Mo are used to define paleo-redox conditions; Si/Al, Ti/Al, Zr/Al are looked at as proxies of clastic influx and C/P is used as proxy for paleo-productivity (Rimmer et.al, 2004).

4.1 Major and Trace Elements

Magnesium (Mg), Aluminium (Al), Silicon (Si), Phosphorus (P), Sulfur (S), Potassium (K), Calcium (Ca), Titanium (Ti), Vanadium (V), Chromium (Cr), Manganese (Mn), and Iron (Fe) is the array of major elements generated and analyzed in this study. The different trace elements generated and studied include Cobalt (Co), Nickel (Ni), Copper (Cu), Zinc (Zn), Thorium (Th), Rubidium (Rb), Uranium (U), Strontium (Sr), Zirconium (Zr), and Molybdenum

(Mo). Trace elements have often been used to infer information about paleoenvironments by various researchers (Dean and Arthur, 1989; Zheng et al., 2000; Rimmer, 2004; Tribovillard et al, 2006; Algeo et al, 2003, 2006; Brumsack, 2006; Algeo and Maynard, 2008; Rowe et al., 2008; Algeo and Tribovillard, 2009; Piper and Calvert, 2009).

4.2 Detrital influx

The Si/Al ratio has been used as a proxy for detrital influx, and is a ratio that represents quartz/clay. (Tribovillard et al, 1994; Caplan and Bustin, 1998; Murphy et al, 2000, Rimmer et al, 2004). **Figure 3.2** affirms the overall silica concentration of 21.605 % (table 3.2) to be slightly higher in the Bossier than the underlying Haynesville shale with 19.76 % silica (**table 3.2**). Silica exhibits a very strong linear trend with aluminum in the Haynesville as shown in **Figure 3.3**, which indicates that the majority of silica in the Haynesville resides in clay fraction. However, the abrupt peaks of Si/Al in **Figure 3.4** and the high silica data points that lie above the silica-aluminum trend line in **Figure 3.3** illustrates that there are other silica minerals apart from clay. The XRD pattern (**figure 3.1**) indicates the presence of notable amount of quartz, and comparatively insignificant quantity of albite in both the Bossier and the Haynesville, which would be the two dominant silica mineral phase apart from clay.

The Bossier deposition has sporadic silica influx in the East Texas Basin whereas the Haynesville shale shows a decreasing trend in silica concentration, which is revealed by **Figures 3.2.** and **3.3.** These abrupt peaks of silica and silica normalized to clay (Si/Al) observed in **Figures 3.2** and **3.4**, both in the Bossier as well as the Haynesville formation probably represent silica influx to the basin in a very short period of time that could indicate eolian inputs, flooding events, or even biogenic silica.

It is not very clear if the excess silica in the lower Haynesville (**figure 3.4)** is detrital or biogenic. However, the presence of biogenic silica in black shales possibly originates from radiolarians (Schieber, 1996), makes Si or Si/Al problematic as an indicator of clastic influx (Schieber et.al, 2000; Rimmer et.al, 2004); hence detrital proxies like Ti and Zr need to be evaluated.

The detrital provenance of any element can be checked by crossplotting with aluminum or titanium, which are commonly detrital and immobile during diagenesis (Tribovillard et al., 2006). Aluminum is an important detrital element and a proxy for clay that is not affected by biological or diagenetic processes (Brumsack, 2006), and is scarce in seawater (Orians and Bruland, 1986, Brumasck, 2006).Titanium or Zirconium have a very low sea-water abundance (Li, 1982), typified by high charge to size ratio and do not participate in biologic cycling; thus any peaks of these elements definitely reflect detrital input (Piper and Calvert, 2009). Any other elements that show linear relationships with Ti or Zr could reasonably be of detrital origin. Ti occurs both in clay and in sand sized grains of ilmenite, rutile and augite (Calvert, 1976; Shimmield, 1992; Rimmer et al., 2004), thus higher Ti/Al may suggest the presence of Ti containing minerals often associated with coarser-grained sediments (Schmitz, 1987; Rimmer et al, 2004). Ti/Al has also been used as a grain size proxy and an indicator or paleo-wind strength (Boyle, 1983; Shimmield 1992, Bertrand et al, 1996, Rimmer et al 2004) and hence sedimentation rate (Murphy et al, 2000; Rimmer et al, 2004). **Figures 3.2** and **3.4** depicts the stratigraphic fluctuation of Ti in both the Bossier and the Haynesville with the average weight percent titanium in the Bossier to be 0.396%, slightly higher than the underlying Haynesville shale with 0.311% Ti (**table 3.2**). Because Ti is contained in heavy minerals like rutile, which are indicative of an energetic coastal depositional system (Dellwig et al., 2000), we can infer a shallower more energetic depositional environment (low stand) depositing siltier Bossier,

compared to the shaleier micritic Haynesville formation deposited in a deeper (highstand) more quiescent depositional period.

Peaks of Silica along with peaks of Ti and Zr at the same stratigraphic depth can indicate detrital silica, since Ti and Zr are terrestrial elements. Considering detrital proxies like wt. percent Si, Ti, Zr and TOC, possible detrital silica has been highlighted in cyan and biogenic silica has been highlighted in grey in **Figures 3.2** and **3.4**. The lower Haynesville evidently constitutes biogenic silica since a rise in the level of the total organic carbon (TOC) is observed that could be the result of a major increase in production (or a shift in community composition) at this time (Sageman, 2002); also demonstrated in **Figure 3.4**.

Iron exhibits a linear relationship with aluminum (**figure 3.8**), indicating the occurrence of Fe in clay. Iron probably resides in Illite and/or the chamosite (Iron rich chlorite end-member) of the chlorite group as pointed out by XRD analysis. However, enrichment of Fe relative to the Fe-Al line indicates the presence of iron in other mineral phases aside from clay.

A crossplot of Fe versus S (**figure 3.6.A**), displays a moderately linear trend, indicating that some Fe exists in sulfides (i.e. pyrite). This inference is also supported by the linear trend of Fe with Ti in **Figure 3.5**, indicating Fe to be detrital just like Ti. The lack of a trend long the siderite line, in a plot of Fe against TIC in both the Bossier and the Haynesville (**figure 3.8G.2**) minimizes the possibility of Fe residing in a carbonate phase. High Sulfur concentrations, or those data points that plot above the pyrite line in **Figure 3.6.A**., could be due to the presence of gypsum as indicated by the XRD analysis (**figure 3.1)**, or possibly sphalerite as there seems to be a moderately positive covariation between zinc and sulfur in **Figure 3.6.B**.

The Ca-rich Haynesville shale grades into a Si-rich, Ca-poor Bossier shale formation, which is observed in the chemostratigraphy (**figures 3.2** and **3.4**), and in the Ca-Al-Si ternary

diagrams (**figure 3.10**). An overall average of ~ 9.317 wt. percent (table 3.2) and peaks of up to ~34.6367 wt. percent calcium in the Haynesville shale is much more calcitic than the overlying Bossier with an average of ~2.8 wt. percent calcium (table 3.2). Almost the entire calcium in the Bossier-Haynesville formation resides in carbonate phase as demonstrated by the linear calcite trend in the calcium against total inorganic crossplot in **Figure 3.9.A.** The XRD analysis (**figure 3.1**) also supports occurrence of calcite in the Bossier-Haynesville.

4.3 Depositional environment

The Bossier-Haynesville deposition can be evaluated temporally, stratigraphically and spatially, by examination of the changes in chemostratigraphy within a core, and between different cores representative of deposition across the ETB. Concentration of several major elements (eg. Ca, Si, Al), enrichment factors, TOC-S-Fe ternary, weight percent or elemental ratios of redox trace elements (eg. Mo, V, Cr), and total Organic Carbon (TOC) concentrations will be carefully studied and interpreted for this purpose.

Redox-sensitive trace elements, such as Mo, Cr, U and V tend to be more soluble in oxidizing conditions and less soluble in reducing conditions making them enriched in anoxic sediments (Tribovillard et al., 2006), and therefore elemental concentrations (e.g. Mo ppm) has been used in studies by different researchers (Pratt and Davis, 1992; Crusius et. Al, 1996; Dean et al, 1997; Rimmer et al, 2004, Rowe and Mainali, in press) to define paleo environments. Their elemental ratios normalized to Al (e.g. Mo /Al) or trace element ratios like Ni/Co, V/Cr and V/ (V+Ni) have been considered to be redox-sensitive (Hatch and Leventhal, 1992; Jones and Manning, 1994) and thus have been studied for the same purpose. These redox proxies especially Mo, V, Zn and U has been reported to be enriched by up to two to three orders of magnitude in black shales relative to those in grey shales, which is similar or even higher than those from modern anoxic/ euxinic environments (Algeo et.al. 2003).

Mo concentrations of 20 to 160 μg/g have been observed in many anoxic basin sediments, including the Black Sea, Cariaco Trench, Framvaren Fjord and Saanich Inlet (Jacobs et al., 1987; Emerson and Huested, 1991; Crusius et al., 1996; Zheng et al., 2000, Algeo and Lyons, 2006; Algeo et al., 2007,), and moderate enrichment of molybdenum tend to indicate sub-oxic deposition (McManus et.al, 2006, Poulson et.al, 2006). Therefore, sedimentary Mo has been, and can be potentially used as a proxy of paleo-euxinia.

In comparison to the overlying Bossier, higher levels of enrichment of Mo is observed in the Haynesville Shale, (**figure 3.2)** until it reaches the indistinct lower Haynesville (Haynesville Lime or could also be the underlying limy Smackover formation) observed in **Figure 3.4.** Average molybdenum concentration in the Haynesville at 20 ppm (**table 3.3**) with peaks of Mo enrichment to up to 185 ppm (in the Elm Grove core) indicate dysoxic to anoxic depositional environment, whereas with an average concentration of Mo of .014 ppm (**table 3.3**) ranged from less than the lowest detection level of the XRF instrument to 8 ppm, the Bossier is definitely deposited during more oxygenated periods.

Moreover, the trace element concentration in the form of Enrichment factor (EF) is used to evaluate the redox character of the Bossier- Haynesville formation. Enrichment factor = **1** represents similar level to that of average crustal abundance, and represents oxic-deposition conditions, while higher EFs (**>1**) represents the number of times of enrichment levels compared to the average crustal abundance and represents anoxic or even euxinic deposition conditions (Calvert and Pedersen, 1993, Crusius et.al, 1996). Any relative enrichment is then expressed by EF**> 1**, and depletions by EF**< 1** (Brumsack, H.J, 2006). High average EF of Mo at ~ 20 represented by vertical brown lines, and EFs > 50 Mo (Algeo et.al, 2003) in the lower Haynesville (**figure 3.12**) is an indication of an anoxia dominated environment turned dysoxic during the course Haynesville shale deposition. Pertinent agreement of enrichment pattern

between EF_{Mo} and other elements like V, Zn, and U, which also have a strong affinity toward anoxia-euxinia (Algeo et.al, 2003, Algeo and Maynard, 2008) revealed in **Figure 3.12,** also supports the idea of Kimmeridgian anoxic turned dysoxic East Texas basin.

4.3.1 Degree of Pyritization

Degree of pyritization (DOP_T) is the ratio of pyritic iron to the total iron (Raiswell et.al, 1988, Rimmer et.al, 2004). DOP_T shows the redox conditions during deposition. The processes of sulfate reduction and pyrite formation are related; therefore organic-rich sediments and rocks tend to show positive correlations among Fe, S, and TOC (Dean and Arthur, 1989).

Degree of pyritization could be approximated with a Fe-S-C diagram as recommended and implied by Dean and Arthur (1989), Arthur and Sageman (1994), and Rimmer et.al, (2004); normal marine samples would plot along a line representing a S/C ratio of 0.4, in a Fe-S- TOC ternary. Samples where all iron was used to form pyrite or samples that contain only pyritic sulfur would plot along the stoichiometric pyritic line (S= 1.15Fe) and have intercept on the iron axis at 0 (because the S/Fe ratio cannot be greater than 1.15 **(**(55.584/119.984) Fe ~ 46.33 % and (32.065*2)/119.984 S ~ 53.45 % in FeS_2**)**. Samples that plot below the pyritic line presumably contain some other form of sulfur addition to pyrite like gypsum and barite (Dean and Arthur, 1989).

DOP_T values less than 0.42 (Rimmer et.al, 2004) or 0.45 (Sageman, 2002) reveal normal marine conditions and DOP values exceeding .75 indicate anoxic and/or euxinic conditions (Sageman, 2002; Rimmer et.al, 2004).

On the Fe-S-TOC ternary diagram (**figure 3.13**), we can see that almost all the Haynesville samples plot between the normal line and the pyrite line. Very few samples plot below the pyrite line, which could be the result of sulfur in gypsum, barite or sphalerite mineral

phases. As discussed earlier, the most likely mineral phase of sulfur other than pyrite would be gypsum, also indicated by the XRD analysis. A majority of mid to top **(figure 3.13)** Haynesville samples plot between the normal marine line and the green line, but an average $DOP_{T\ mid\text{-}top}$ can be inferred from those samples that cluster around the orange line with a DOP_T value of 0.63.The bottom Haynesville samples tend to plot between normal marine line and the pyritic line, but overall cluster around the blue line that represents an average $DOP_{T\ bottom}$ value of 0.78.

Degree of pyritization (DOP_T) of the Haynesville (Elm Grove Core) ranges from 0.1 to 1.4, with an average value at 0.5 indicating borderline dysoxic-anoxic. This wide range of DOP_T values places Haynesville bottom water conditions to be anywhere between oxic to anoxic levels, and the average Haynesville ($DOP_T = 0.5$) to be of dysoxic or anoxic levels. Stratigraphic variation of DOP_T along with enrichment factor EF of Mo, and TOC content in the Elm Grove core is presented (**figure 3.14**). Using proxies of anoxia like EF_{Mo}, DOP_T, V/Cr and TOC, the likely anoxic intervals are highlighted in red in **Figure 3.14**.

The same Figure 3.14 also exhibits the prevalence of anoxic/ euxinic environment (highlighted in red) during early Haynesville deposition that turned largely dysoxic during middle to upper Haynesville times, with some probable very short oxic intervals during upper Haynesville periods highlighted in blue. Rapid siliciclastic sedimentation even under anoxic/euxinic conditions could cause the DOP_T values to read low, wrongly suggesting oxic conditions (Sageman, 2002). But rapid sedimentation could also mean higher concentrations of silica. That is not the case as clarified by plotting wt. percent silica of the same core (**Figure 3.14**), which suggests there are reoccurring short intervals of oxic environments during the latter period of Haynesville deposition.

Like Ti, Cr is also associated only with the detrital faction (Dill, 1986; Rimmer et al 2004), and is not influenced by redox conditions (Rimmer et al., 2004), therefore V/Cr >4.25 are

thought to indicate anoxic conditions (Jones and Manning, 1994; Rimmer et al, 2004). Positive covariation between high V/Cr concentration and other anoxic proxies can be observed in **Figure 3.14**. The lower Haynesville samples plot above or close to the anoxic cut-off line of 4.25 represented by the vertical red line, compared to the mid-top Haynesville samples.

Berner (1970, 1982) and Leventhal (1983) have established a good correlation between organic carbon and $sulfur_{pyrite}$ in modern marine sediments (Berner and Raiswell, 1983). Crossplots of TOC-S have been used by Berner and Raiswell (1983), and Rimmer et.al. (2004) to distinguish between normal marine (Oxic) from anoxic/euxinic environments, because oxygenated sediments (normal marine sediments) show a positive correlation between organic carbon and pyritic sulfur. Data points plotted on the left of the normal marine line on a cross plot of sulfur against TOC is another indication of an anoxic regime during Haynesville deposition (**figure 3.15**). A sulfur rich bottom Haynesville compared to the middle and the upper Haynesville is yet another indicator of an anoxic to a dysoxic depositional environment during the upper Jurassic Haynesville times.

The observations made in the trace metal enrichment in the form of EF (**figure 3.12**), the Fe-S-C ternary (**figure 3.13**), the stratigraphic DOP_T values (**figure 3.15**), the crossplot of TOC-S (**figure 3.15),** all support the previously stated hypothesis of an anoxic turned dysoxic environment during the Bossier-Haynesville deposition in the late Jurassic (Kimmeredgian-Tithonian) East Texas Basin.

4.3.2 Basinal restriction and deep-water renewal time

Algeo and Lyons (2006), Algeo et al, (2007), and Rowe et al., (2008) have associated the basinal hydrographic restriction to deep water renewal time, where they have asserted that the basin gets more restricted with a longer deep-water renewal time, and the Mo/TOC ratio in such sediments decreases. Algeo and Lyons (2006), and Algeo et al., (2007) have demonstrated the Mo/TOC ratio of the four most studied modern silled anoxic marine basins, Saanitch Inlet (British Columbia), Cariaco Basin (Venezuela), Framvaren Fjord (Norway), and the Black sea (Eurasia). Rowe et al., (2009) have added the Fort Worth Basin (FWB) into the graph, in their extensive chemostratigraphic study on the Mississippian Barnett Formation of the FWB.

The method is based on the observation that the concentration of Mo in anoxic sediments depends on the concentration of the host phase (i.e. sedimentary organic matter), and concentration of Mo in the marine water (Algeo and Lyons, 2006; Algeo and Rowe, in press).

If the basinal aqueous molybdenum concentration is high, then the (Mo/TOC) ratio is higher. Aqueous Mo can be high under unrestricted conditions and rapid deep water renewal (Algeo and Rowe, in press). Restricted basins such as the Black Sea have lower Mo/TOC slopes (~ 4.5), partially restricted basins such as Framvaren Fjord and the Cariaco basin have average Mo/ TOC slopes of 9 and 25 respectively, and the less restricted Saanitch Inlet has a m~45 (**figure 3.16**).

The redox conditions of the late Jurassic East Texas Basin can be further understood by studying similar cross-plots of Mo against TOC of the Bossier-Haynesville shales. On such a cross-plot of Mo against TOC, the Haynesville samples of the eastern ETB (**figure 3.16 c** and

d) plot between the lines that define the Saanich Inlet and the Cariaco Basin, and indicate a limited restricted basin with a deep-water renewal time of less than 100 years (Algeo et al., 2008). Whereas the samples from the western part of the basin represented by the Huffman and the USA Double cores (**figure 3.16 a** and **b**), could indicate one of the two things, 1.) Either an increased basin restriction with a deep water renewal time of several thousand years (Algeo et al., 2008, Algeo and Maynard, 2008), since the Mo-TOC line plots between the lines that define Black-sea and the Mississippian Barnett Formation of the Fort-worth basin, or 2.) The low Mo concentration in the western ETB is associated with water depth. In that case, the Mo vs. TOC in the western-ETB does not form a linear trend, but is clustered at the bottom because of low Mo concentration in oxygenated shallow watered condition during deposition. An east-west cross section of the ETB reveals the increasingly higher Mo concentration in the eastern-ETB (**figure 3.17)**, indicating deeper depositional conditions. Moreover, the Mo-TOC relationship is strongest in the easternmost cores (**figure 3.16 c** and **d**), representing the deepest and the most distal depositional conditions (Rowe and Mainali, in press). In addition to that, the Ca-Al-Si ternaries (**Figure 3.13**) display comparative clay rich Haynesville shale in the eastern part of the East Texas Basin presumably indicating an eastwardly deepening ETB.

Furthermore, the TOC generated from the Bossier-Haynesville core samples are lower than the original TOC values, because the analyzed Haynesville shale has undergone hydrocarbon generation. Thus if the original TOC could be estimated, the $Mo/TOC_{original}$ would be lower, and the estimates of the deep-water renewal time for the basin would be larger (Rowe and Mainali, in press), a more restricted basin.

4.4 Paleo-productivity Proxies and the role of productivity in redox control

Terrestrially derived nutrients that were ultimately delivered to the ocean can contribute to high surface water productivity that in turn can result in excess benthic oxygen demand, producing anoxic bottom water (Algeo et al, 1995; Rimmer et al, 2004), suitable for the preservation of organic matter (Demiason and Moore, 1980). Moreover, the TOC content of sediments is the residue of the past biota (Meyers, 1997), and thus productivity has a direct relationship with organic matter preservation. Accumulation of organic carbon seems to have a direct relationship with productivity and nutrients availability (especially P) in the surface water (Rimmer et. al., 2004). Pedersen and Calvert (1990), and Sageman et al, (2002) have suggested that high primary production also controls ancient organic matter burial, as in the Peru shelf where the high influx of organic matter raining down the water column is important in maintaining O_2 depletion. High productivity (Codispoti, 1980; Chavez and Barter, 1987) could be driven by upwelling (Piper and Perkin, 2004). The vast temperature difference between the land and ocean in a warmer interglacial period like the late Jurassic can activate seasonal upwelling, and as a result high productivity (Algeo et al., 2008). Good Correlation between % P and % TOC (**figure 3. 18**) indicates high nutrients in samples with high organic carbon, and could be concluded as being the result of high primary productivity.

In a study of the same aged Kimmeridgian clay formation of United Kingdom, the control on the clays composition has been attributed to marine productivity and preservation (Pearce et al., 2010). Both low oxygen content with high productivity is the key to high organic matter preservation, evidential in the Bossier of **Figure 3.18**. Highlighted in blue are high productivity zones (indicated by high P content), but relatively low accumulation of organic carbon probably due to the more oxygenated waters during Bossier deposition. Comparatively higher percent

TOC during the Haynesville (highlighted in red) is attributed to high productivity as indicated by high concentration of P, and anoxic to euxinic water conditions.

4.4.1 Organic matter provenance

The average percent total organic carbon (TOC) of the Bossier shale is .574 % (**table 3.1**) but ranges from .323 % - 2.39 % and the average TOC of the Haynesville is 2.917% (**table 3.1**) ranged from .54 % - 6.46 %. The $\delta^{13}C$ values ranged from -28.58 $^{o}/_{oo}$ to -26.33 $^{o}/_{oo}$ with an overall average of -26.904 $^{o}/_{oo}$ (**table 3.1**) for the Bossier shale, and the $\delta^{13}C$ values for the Haynesville ranged from -27.8 $^{o}/_{oo}$ to -24.9 $^{o}/_{oo}$ with an overall calculated average of -26.271 $^{o}/_{oo}$ (table 3.1). Organic matter produced by land plants (using atmospheric CO_2) has an average $\delta^{13}C$ value of approximately -27 $^{o}/_{oo}$, whereas marine organic matter (algae uses dissolved bicarbonates as inorganic carbon), has $\delta^{13}C$ values between -20 $^{o}/_{oo}$ to -22 $^{o}/_{oo}$ (Meyers, 1994,1997). This difference of ~7 $^{o}/_{oo}$ between organic matter produced from land plants and marine algae has been used successfully to trace organic matter source and distribution in coastal ocean sediments (Prahl et al., 1994; Meyers, 1997).

The C/N values range from 3.2 to 23.7 but averages at 8.8 for the Bossier Shale. Values for C/N in the Haynesville range higher, from 8 to 47, with a cumulative average of 23.509.Typically marine algae have C/N ratios between 4 and 10, and land plants have a higher C/N ratio of 20 and greater (Meyers, 1994, 1997).

The provenance of the organic matter of the Bossier-Haynesville cores was examined using organic carbon and carbon-nitrogen ratios (C/N), on a plot of C/N vs. $\delta^{13}C$ developed by Mayers (1997). The Bossier organic matter was determined to be a mixture of lacustrine and marine algae type with a huge terrigenous component (**figure 3.19**). The organic matter in the Haynesville according to Meyers (1997) is of vascular terrestrial plants.

$\delta^{15}N$ in sediments can also be used as a proxy to distinguish between marine-algal and terrestrial-plant sources of the organic matter. This distinction is made possible because the $\delta^{15}N$ value of dissolved nitrate (source of inorganic nitrogen for marine algae) ranges between $7^{o}/_{oo}$ to $10^{o}/_{oo}$, whereas $\delta^{15}N$ of atmospheric N_2 (source of inorganic nitrogen for land plants) is ~$0\,^{o}/_{oo}$ (Peters et al., 1978; Meyers, 1997).

Figure 3.20 is a plot of $\delta^{15}N$ vs. $\delta^{13}C$, also used by Meyers (1997) to trace organic matter sources. Both the Bossier and the Haynesville show signs of organic matter in the sediments derived from C3 land plants.

Though Bossier-Haynesville shale is a marine deposit as discussed earlier in the introduction section, why is the isotopic analysis indicating a more terrestrial influence in the accumulation of organic matter in the Bossier-Haynesville formation?

A higher C/N ratio could be the result of selective degradation of nitrogen by microbial organisms or nitrogen fixing algae (Peters et al., 1978; Rau et al., 1987, Werne et al., 2002, Algeo et al., 2008b); therefore high C/N ratios are often seen in areas with high primary productivity (Meyers, 1997; Twichell et al, 2002). High productivity resulting in denitrification during Bossier-Haynesville deposition may have caused the high C/N ratio. Positive covariation between C/N ratio with productivity proxies and TOC (**figure 3.18**) in the Haynesville shale supports selective degradation for high C/N ratio, and thus falsely mimicking C3 vascular plant origin of organic matter though it very likely is of a marine algal derivation.

A reason for the low $\delta^{13}C$ to read and imitate organic matter derived from land plants could be because there could have been a higher concentration of CO_2 in the atmosphere (than the present) (Berner, 1994). If that was the case, then the OM content of the Bossier-

Haynesville shale could have wrongly indicated terrestrial origin just like the Eagleford Samples in **Figure 3.20** (Dean et al., 1986; Meyers, 1989, 1997).

4.5 Multi-proxy Sequence Stratigraphy of the Haynesville Shale

Sequence stratigraphy attempts to explain the nature of basin fills in terms of relative sea-level changes (Taylor and Sellwood, 2002). Assigning stratigraphic sequences and their system tracts in shale and mudrock strata can be difficult due to the overall lithologic homogeneity and the very fine grained nature of the rock (Ver Straeten et al, 2010). In which case, a multi-proxy geochemical approach could aide in delineating these stratigraphic surfaces.

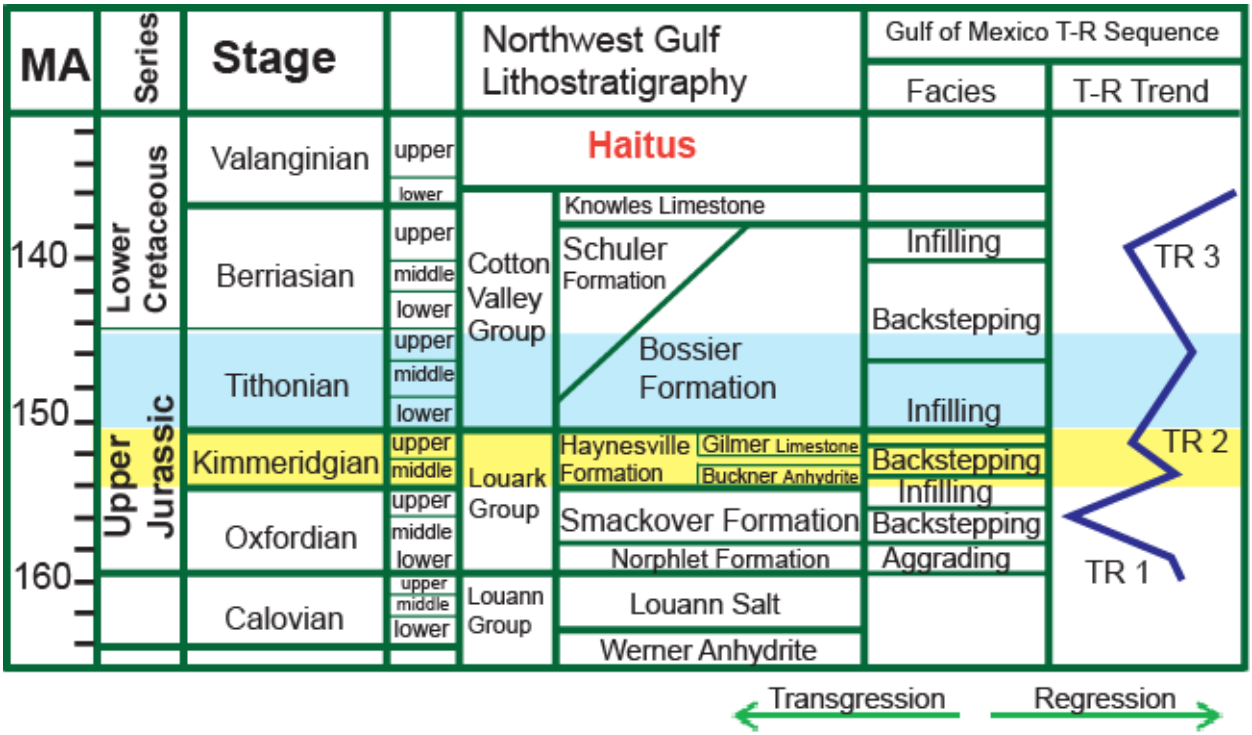

Figure 4.1 East Texas Basin (ETB) absolute ages, lithostratigraphic units, and transgressive-regressive sequences (after Mancini et al., 2004; McGowen and Harris, 1984).

It has been interpreted that the Haynesville and the Bossier were deposited in a time of rising sea level, a part of a second order eustatic cycle that probably began in the mid-Jurassic (Haq et al., 1987; Hallam, 1988; Hammes et al., 2011) as illustrated by two different research groups in figure 4.2. Although the Haynesville shale lies within a global 2nd-order transgression (Hallam, 1978, 2001; Hammes and Frebourg, 2011), at least three T-R sequences of possibly 3rd-order (within 7 to 8 million years in duration) can be identified in the upper Mesozoic (Oxfordian to Berriasian) beds of the East Texas Basin (northern Gulf of Mexico Basin) (Mancini et al., 2004). The three transgressive- regressive trends of the East Texas Basin (northwest Gulf of Mexico) is shown in figure 4.1.

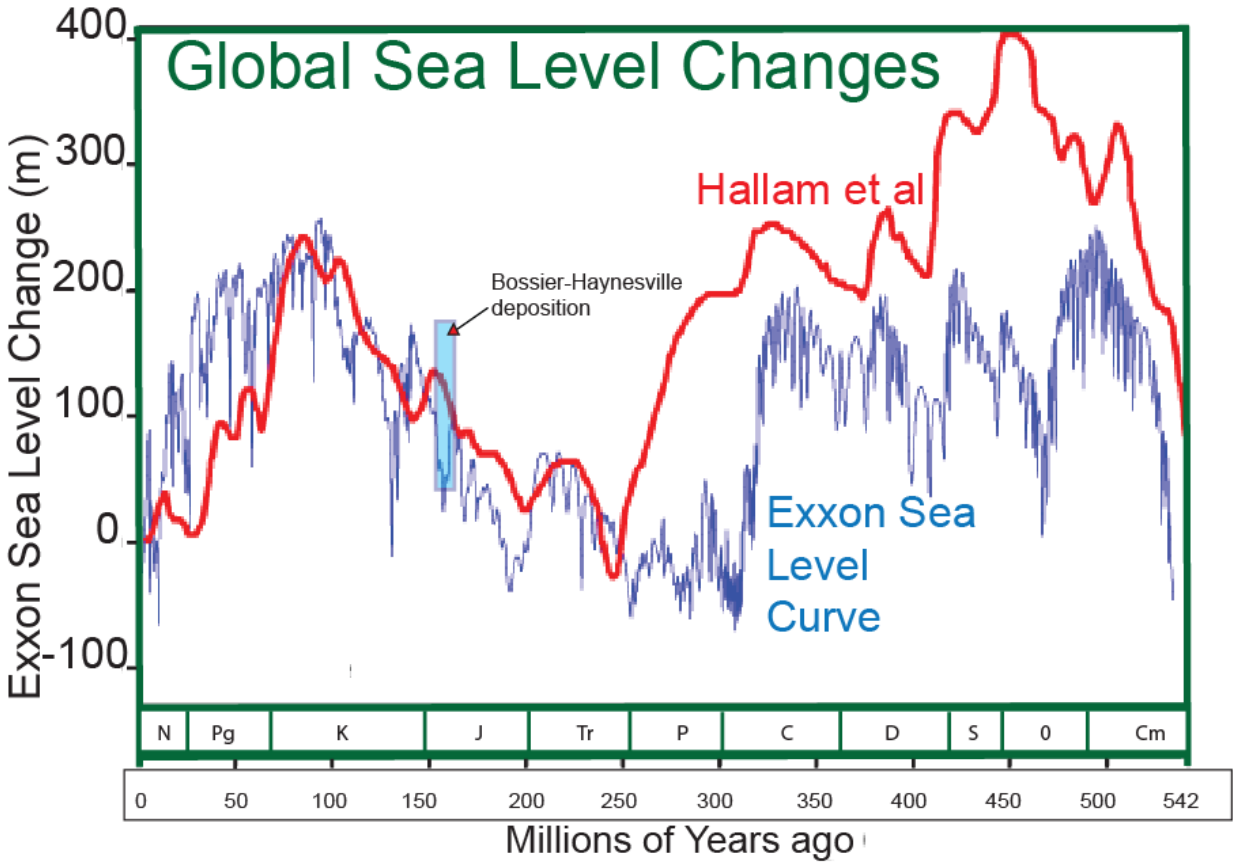

Figure 4.2 Global sea-level changes from Exxon Research Group and Hallam et al.

The following represents an attempt to conjoin chemostratigraphy and sequence stratigraphy of the Bossier- Haynesville system of East Texas, and is not intended for any detailed sequence stratigraphic interpretation of the East Texas Basin. It is meant to represent a comparison of the transgressive-regressive trends observed by previous researchers in the ETB (GOM) to the trends observed in the chemostratigraphic data. For this purpose, the T.W. George core (Harrison County, TX) was selected for three reasons: 1) the cores proximity to the shelf and therefore principles of sequence stratigraphy were more applicable, 2) the core include parts of the Tithonian Bossier shale and 271.25 feet of the Haynesville, 3) the availability of wells logs and core descriptions (courtesy of Dr. Ursula Hammes, Texas Bureau of Economic Geology, The Jackson School of Geoscience, University of Texas, Austin.)

Due to the variable paleoceanographic and paleoecologic conditions, and variable diagenesis after deposition, the selection of geochemical proxy for the purpose of delineating sequences varies. A tentative but feasible model is drawn in figure 4.3 for the upper-Jurassic Bossier-Haynesville shale deposition, after the recognition of the provenance, and the redox nature of the geochemical proxies. In the case of anoxic-dysoxic basinal facies such as those preserved within the Haynesville, sedimentary proxies like Mo and, TOC can be used (Werne et al., 2002; Ver Straeten et al., 2010), whereas for the dysoxic-oxic clastic Bossier, proxies like Si, and bioturbation are best for purposes of delineation and correlation (Ver Straeten et al, 2010). In particular for the Jurassic ETB, siliciclastic deposition dominated the North and the East, and carbonate production dominated in the South and the West (Goldhammer, 1998; Ewing, 2001, 2009; Hammes et al., 2011), therefore Ca is a strong detrital indicator in the South and the West of the basin, and Si is better in the North and north-east sectors of the ETB. As discussed earlier, Si can be affected by biogenic contributions, eolian and even volcanogenic sources (Sageman and Lyons, 2003). Therefore a multi-proxy approach is suggested and implied, where

multiple evidences are evaluated before deducing the position within sequences. A geophysical log (Gamma ray) and core description is utilized for comparison and interpretation.

Geochemical proxies of Si/Al, Ti/Al, Zr/Al, Al, TOC and bioturbation can be used to identify position within a sequence (Ver Straeten et al., 2002) because they serve as a proxy for either one of the system tracts. Siliciclastic input is expected to be higher during lowstand due to an increased amount of terrestrial input attributed to winnowing of the land during lower sea levels, and a higher degree of bioturbation is expected in shallow oxygenated water (Loucks and Ruppel, 2007). In particular with the Kimmeridgian ETB, the cessation of the carbonate factory during lower sea-levels increases the relative Si being deposited. With the assumption that %Al is a stratigraphic proxy for % clay, we define Si/Al ratio as an indicator of quartz/clay regardless for the origin of the quartz. Therefore Si/Al > 5 can be used as a proxy for sand-dominated lithology (Ver Straeten, 2002) of a lowstand system. Bulges or isolated peaks of Si/Al probably indicate non riverine detrital silica, e.g. eolian, biogenic bloom or volcanic. Fluvial or riverine input is generally an increasing Si trend, unless it is a flooding event.

The presence of hydrocarbons in the Haynesville shale, suggests that water depth in the ETB was deep enough to allow persistent stratification of the water column (Tyson et al., 1979; Taylor and Sellwood, 2002), also indicated by the presence of framboidal pyrite (Hammes et al, 2011.), trace elements such as, molybdenum, and vanadium (Werne et al., 2002); Rimmer et al., 2004; Algeo and Lyons, 2006; Rowe et al, 2008), high degree of pyritization (DOP) (Raiswell 1986, 1988; Algeo et al., 2008b), and sediment laminations seen in the core description, which would have been destroyed by bioturbation in an aerobic shallow water setting. Several proxies like TOC, trace element concentrations and degree of pyritization (DOP) exhibit symmetrical cycles (Algeo et al, 2008b), low values at both the transgressive and regressive phases, but reach a maximum value at or near the maximum flooding surface (MFS). Variations in theses

proxies very likely was controlled mainly by depth-related changes in the benthic redox conditions, with increasing depth leading to a more anoxic condition, and a higher proxy value (Algeo et al., 2008b). Also discussed earlier, is the use of Mo as a proxy for deep water anoxia (Zheng et al., 2000; Algeo and Lyons, 2006; Rowe et al., 2008; Pearce et al., 2010), and thus Mo can be used as an indicator of deep-water anoxic conditions of a probable Highstand system. Sea level rise is an important factor in TOC enrichment in shelfal depositional environments such as the Kimmeridgian ETB (Arthur and Sageman, 2004).Because Mo, TOC and anoxia is interrelated (Sageman and Lyons, 2003; Tribovillard et al., 2006), they can jointly be used to show eustatic rise.

Table 4.1 List of proxies used to differentiate different sequence boundaries of late Jurassic East Texas Basin

Lowstand System (Sand)	**Transgressive System** (Sandy shale)	**Maximum Flooding Surface** (shale)	**Highstand System** (Shale)
High detrital elements (Si, Ti, Zr)	Decrease in Si, Ti, Zr	Low Si, Ti, Zr	Low Si, Ti, Zr
Low % TOC	Increasing %TOC	Peak in %TOC	High % TOC
Low Mo (ppm)	Increasing TOC	Peak in Mo (ppm)	High Mo (ppm)
Low DOP	Increasing DOP	Maximum DOP	High DOP
Bioturbation	Decrease in Bioturbation	No Bioturbation	No Bioturbation

A 2nd order transgressive deposit, the Haynesville is capped by the maximum flooding surface (MFS) (Goldhammer, 1998; Hammes et al., 2011). This surface marks the maximum

extent of transgression, succeeded by the regressive upper Jurassic - Cretaceous succession indicated by the decreasing gamma ray activity (cleaning up trend) reflecting a shale-rich to a shale-free lithology in figure 4.4 (Taylor and Sellwood, 2002).

On the contrary, with less than 400 feet of core available for analysis on the longest core (i.e. T.W. George) at a resolution of one foot intervals, the chemostratigraphic cycles are of a higher order. The analyzed Bossier-Haynesville cores represents less than 6-7 million years of deposition, which covers just a part of the second order sequences with duration of 10 to 80 Myr (Vail et al., 1977), making the second order sequences unrecognizable. Subtle but certain, segments of the 3rd order transgressive-regressive trends of the Gulf of Mexico (after Mancini et al, 2004) can be recognized with the geochemical trends (GR TR1 – GC TR3). These sequence boundaries and system tracts are picked based on the geochemically defined T-R cycles, and the standard sequence stratigraphic mapping methods (Posamentier and Allen, 1999; Catuneanu et al., 2009) (**Figure 4.4)**

The smaller chemostratigraphic T-R cycles (denoted by 4th T-R in **Figure 4.4**) seen within the 3rd order T-R trends confirm that these geochemical cycles are of a higher order, at least 4th order stratigraphic surfaces. These 4th order cyclothems are picked in figure 4.4, but designating different stratigraphic surfaces within these cycles is not attempted in this paper. These higher frequencies are missed, because they are amalgamated within a single 3rd order reflection (Catuneanu et al, 2009). Therefore to observe these stratigraphic surfaces, they have to be mapped at their particular hierarchical level. These smaller scale fluctuations are not always related to eustacy, but also to local tectonic, climatic conditions and paloegeographic settings that can influence progradation and clastic influx.

The geochemical transgressive-regressive cycles though cannot be traced back to the larger 2nd order cycles at this resolution, but can definitely be linked to the 3rd order localized

trends that seem to be predominant at this level of high resolution work. A regional chemo-sequence stratigraphic framework incorporating chemostratigraphic logs to attain lateral extensiveness of the Haynesville is also accomplishable, if complete thickness of different Haynesville cores from around the ETB are analyzed, and a regional surface can be selected as the datum. As in the case of the calcareous Haynesville, an omnipresent Calcium peak is assigned as the datum for regional correlation (**Figure 4.5**). A geochemical correlation between T.W. George core (Harrison, TX) and the Elm Grove core (Bossier Parish, LA) is attempted in figure 4.5.

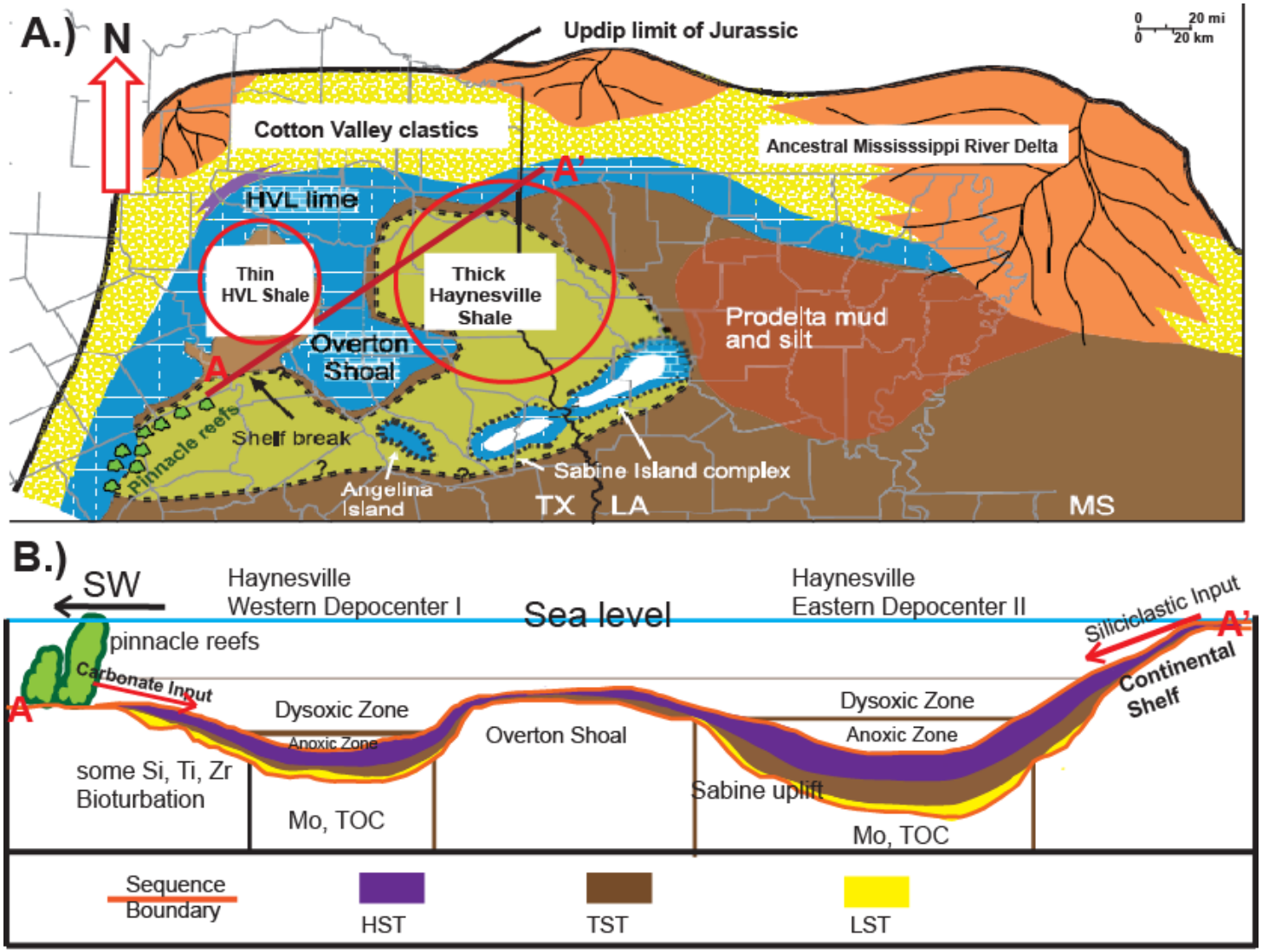

Figure 4.3 A model of geochemical proxy recognition and utilization for the Kimmeridgian Haynesville shale of the silled East Texas Basin. Cross-section line A - A' of figure A.) is displayed in a cross-section view in figure B. (after Ver Straeten, 2010; Figure A from Hammes et al., 2011). Figure not to scale.

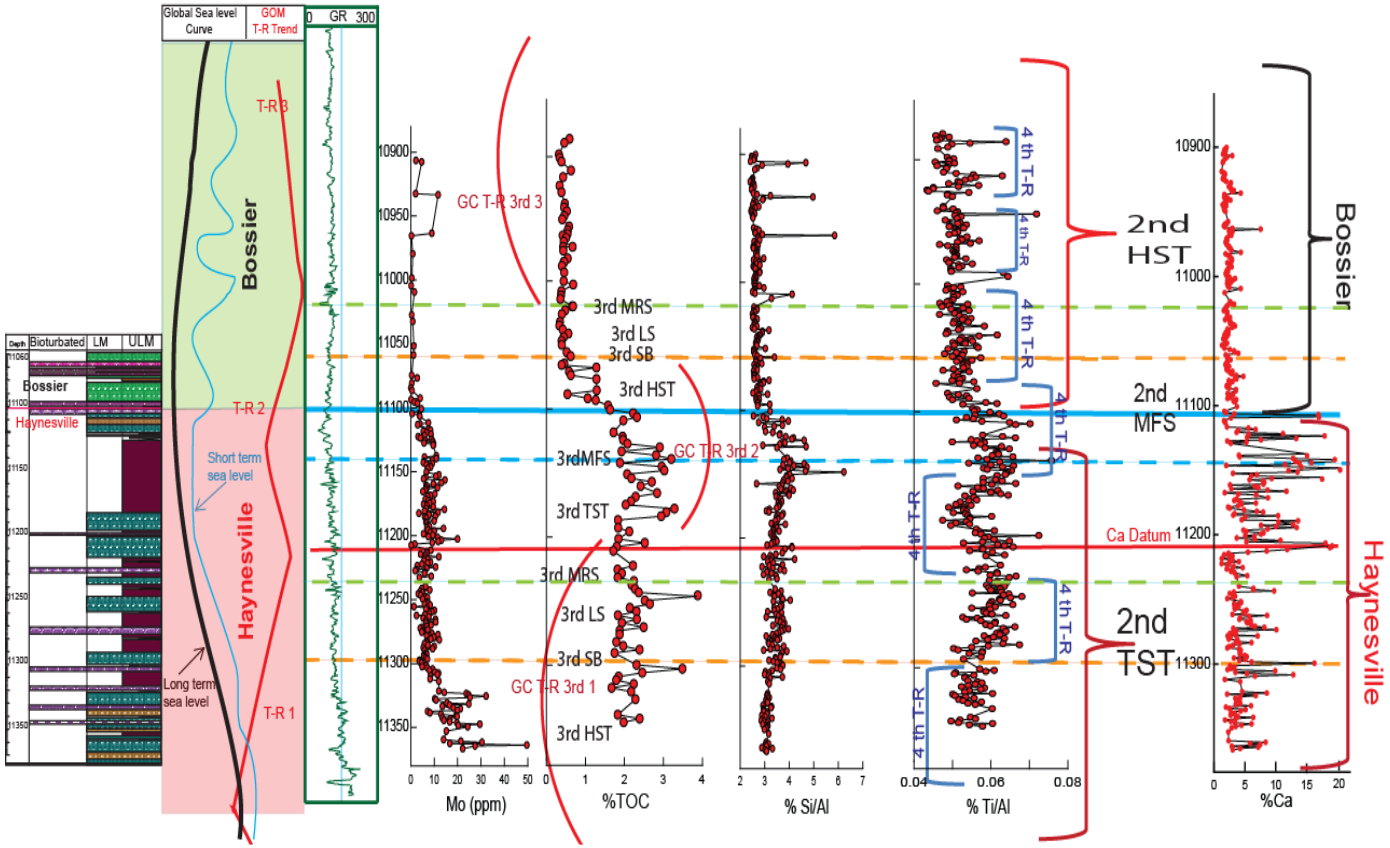

Figure 4.4 Chemostratigraphy and proxy trend of the T.W. George Core. Relative sea-level curve after Goldhammer and Johnson, 2001, and 3rd Order T-R trends (after Mancini et al, 2004). Biostratigraphy provided by Dr. U. Hammes (BEG). GC TR 3rd = 3rd order Geochemical transgressive-regressive trends. 4th T-R = 4th order Geochemical transgressive-regressive cycles. LS= Lowstand system tract, TST= Transgressive system tract, HST= Highstand system tract, MRS= Maximum Regressive surface, SB= Sequence Boundary (Posamentier and Allen, 1999; Catuneanu et al., 2009).

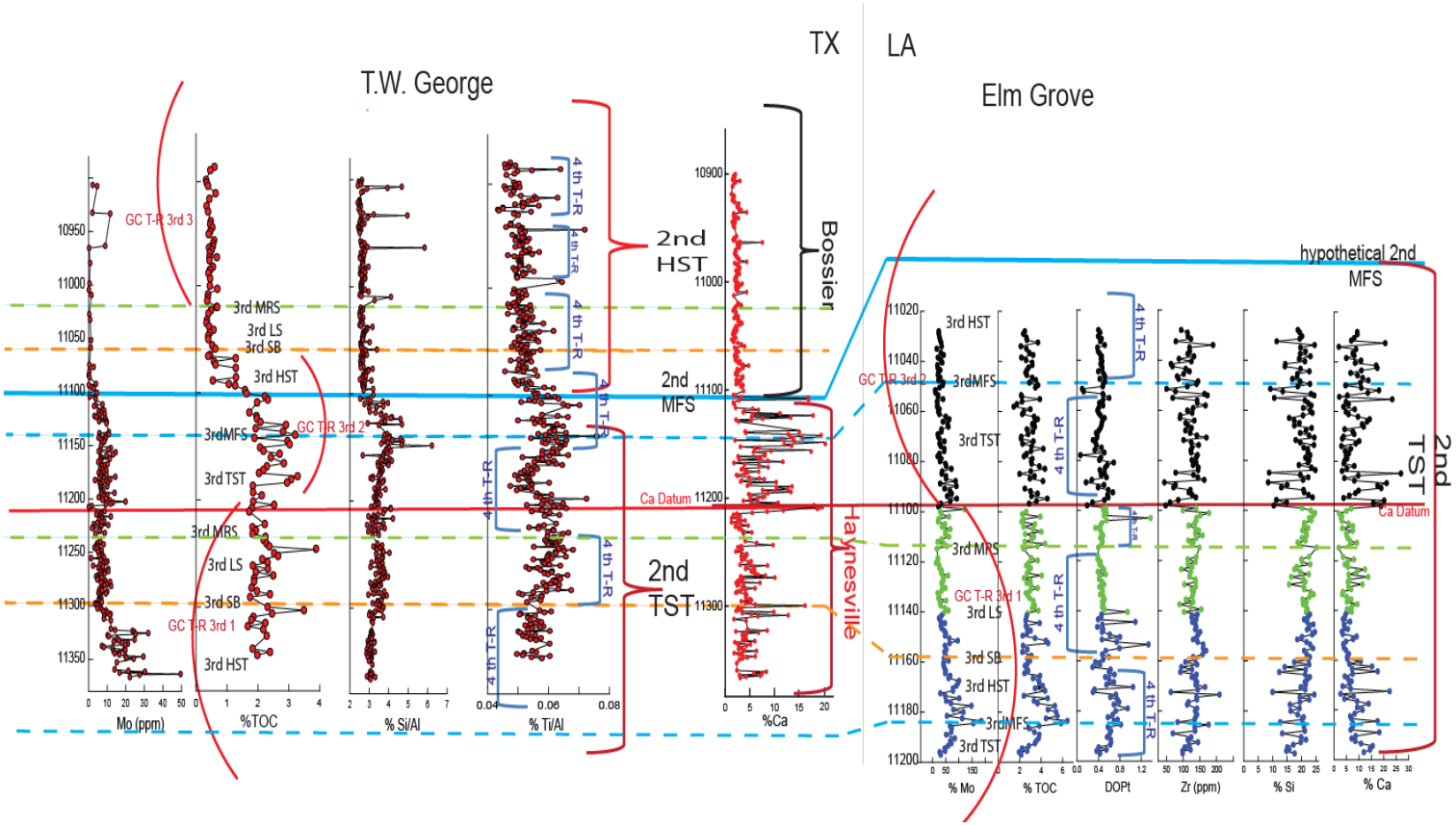

Figure 4.5 Geochemical correlations between T.W. George core (Harrison County) and the Elm Grove Core (Bossier Parish) with the use of the calcium datum (solid red line).

CHAPTER 5

CONCLUSIONS

5.1 Conclusions

Geochemical data is used to reconstruct the chemostratigraphy of the Bossier-Haynesville formations in the East Texas Basin. Geochemical proxies have been used to reconstruct the Paleoceanography of the Kimmeridgian-Tithonian Bossier-Haynesville formation of ETB.

The utilization of geochemical characteristics demonstrated:

1. The strong association of silica with clay in both the calcitic Haynesville and the carbonate-poor Bossier formations, although other mineral forms of Si (mostly quartz) is also present in these shale formations.

2. Si, Ti and Zr analysis indicate some biogenic silica in the both the Bossier-Haynesville formations, but detrital silica dominates in the Bossier but not in the Haynesville.

3. The Bossier-Haynesville Formation was under anoxic to euxinic conditions during Haynesville shale deposition and more oxygenated (dysoxic-oxic) waters during the Bossier.

4. The ETB (the area of the Bossier-Haynesville deposition) was hydrographically restricted with ~ 100 years of deep-water renewal time, based upon Mo/TOC ratios. The western ETB could have been more restricted than the eastern ETB.

5. The Bossier-Haynesville formation is organic matter rich, with an average TOC of .57 % in the Bossier and 2.92% in the Haynesville shale The organic matter was determined to be primarily lacustrine-marine algal origin based on stable isotope ratios for the Bossier. The provenance of OM in the Haynesville though mimicked to be from terrestrial plants is probably from marine algae as well; a result of selective degradation of N by micro-organisms or nitrogen fixing algae, and probably because of higher atmospheric CO_2 concentrations during the Kimmeridgian.

6. Although the Haynesville was deposited during a 2^{nd} order transgression, and the MFS separates the Haynesville shale from the Bossier, the 2^{nd} order cycle was not traceable with the available geochemical data. However, parts of the previously researched 3^{rd} order sequences (Mancini et al., 2004) in the GOM was recognized in the geochemical trends observed. Even higher orders (at least 4^{th} order) eustatic cycles were observed. A geochemical correlation with the different stratigraphic surfaces is possible if a regional datum can be picked.

REFERENCES

Ahr, W.M., 1973. The Carbonate ramp: an alternative to the shelf model: Gulf Coast Assoc. Geol. Soc. Transactions, v.23; 221 – 225.

Andrew, A.S, Whitford, D.J., and Hamilton, P.J., 1996. Application of chemostratigraphy to petroleum exploration and field appraisal: An example from the Surat Basin, Society of Petroleum Engineers, Document ID 37008-MS, SPE Asia Pacific Oil and Gas Conference, 28-31 October 1996, Adelaide, Australia, 978-1-55563-419-3.

Algeo, T.J., Schwark, Lorenz, Hower, James C., 2003 (accepted). High-resolution geochemistry and sequence stratigraphy of the Hushpuckney Shale (Swope Formation, eastern Kansas); implications for climate-environmental dynamics of the Late Pennsylvanian Midcontinent Seaway. Chemical Geology 206 (2004); 259-288.

Algeo, T.J., Lyons, T.W., 2006. Mo-total organic carbon covariation in modern anoxic marine environments: implications for analysis of paleoredox and paleohydrographic conditions. Paleoceanography, v. 21, PA1016, doi: 10.1029/2004PA001112, 2006.

Algeo, T.J., Lyons, T.W., Blakey, R.C., Over, D.J., 2007. Hydrographic conditions of the Devono-Carboniferous Seaway inferred from sedimentary Mo-TOC relationships. Paleogeography, Paleoclimatology, Paleoecology 256; 204-230.

Algeo, T.J., and Maynard, J.B., 2008. Trace-metal covariation as a guide to water-mass conditions in ancient anoxic marine environments, Geosphere, V.4; no.5; 872- 887.

Algeo, T., Rowe, H., Hower, J.C., Schwark, L., Herrmann, A., Heckel, P., 2008. Changes in ocean denitrification during Carboniferous glacial-interglacial cycles, Nature Geoscience Vol 1. Macmillan Publisher Limited.

Algeo, T.J., Tribovillard, N. 2009. Environmental analysis of paleoceanographic systems based on molybdenum-uranium covariation. Chemical Geology. 268; 211-225.

Arthur, M.A., Sageman, B.B., 1994. Marine Black Shales; a review of depositional mechanisms and significance of ancient deposits. Annu. Rev. Earth Planet. Sci. 22; 499-551.

Arthur, M.A., Sageman, B.B., 2004. Sea-level control on source-rock development: Perspectives from the Holocene Black Sea, the Mid-Cretaceous Western Interior Basin of North America, and the Late Devonian Appalachian Basin. In Harris, N.B., (Ed.), The Deposition of Organic-Carbon-rich Sediments: Models, Mechanisms and Consequences. SEPM Special Publication 82; 35-59.

Beall, R, 1975. Plate Tectonics and the origin of the Gulf of Mexico: Gulf Coast Association of Geological Societies Transactions, v.23; 109 – 114.

Berner, R.A., 1978. Sulfate reduction and the rate of deposition of marine sediments. Earth Planet, Sci.Lett. 37; 492-498.

Berner, R.A., 1982. Burial of organic carbon and pyrite sulfur in the modern ocean: its geochemical and environmental significance, Amer.J.Sci. 282; 451-473.

Berner, R.A. and Raiswell, R., 1983. Burial of organic carbon and pyrite sulfur in sediments over Phanerozoic time: a new theory, Geochimica et Cosmochimica Acta Vol. 47; 855-862.

Berner, R.A., 1994. Geocarb II: A revised model of the atmospheric CO2 over Phanerozoic time. Am. J. Sci., 294; 56-91.

Brumsack, H.J. 1989. Geochemistry of recent TOC-rich sediments from the Gulf of California and the Black Sea. Geologische Rundschau 78/3; 851-882.

Brumsack, H.J., 2006. The trace metal content of recent organic carbon-rich sediments: Implications for Cretaceous black shale formation, Elsevier, Paleogeography, Paleoclimatology, Paleoecology 232; 344-361.

Burke, K., Dewey, J.F., 1973. Plume-generated triple junctions: key indicators in applying plate tectonics to old rocks: Journal of Geology, v.81, no.4; 406 – 433.

Caplan, M.L. and Bustin, R.M., 1998. Paleoceanographic controls on geochemical characteristics of organic-rich Exshaw mudrocks: role of enhanced primary productivity. Org. Geochem. 30; 161-188.

Calvert, S.E., 1976. The mineralogy and geochemistry of near-shore sediments. In: Riley, J.P., Chester, R. (Eds.), Chemical Oceanography, vol.6. Academic Press; 187-280.

Calvert, S.E. and Pedersen, T.F., 1993. Geochemistry of Recent oxic and anoxic marine sediments: implications for the geological record. Mar. Geol. 113; 67-88.

Catuneanu, O., Abreu, V., Bhattacharya, J.P., Blum, M.D., Dalrymple, R.W., Eriksson, P.G., Fielding, C.R., Fisher, W.L., Galloway, W.E., Gibling, M.R., Giles, K.A., Holbrook, J.M., Kendall, C.G.St.C., Macurda, B., Martinsen, O.J., Miall, A.D., Neal, J.E., Nummedal, D., Pomar, L., Posamentier, H.W., Pratt, B.R., Sarg, J.F., Shanley, K.W., Steel, R.J., Strasser, A., Tucker, M.A., Winker, C., 2009. Towards the standardization of sequence stratigraphy, Elsevier, Earth Science Reviews 92; 1-33.

Cicero, A.D., Steinhoff, I., McClain, T., Koepke, K.A., and Dezelle, J.D., 2010. Sequence stratigraphy of the Upper Jurassic mixed carbonate/siliciclastic Haynesville and Bossier shale depositional systems in east Texas and northern Louisiana: Gulf Coast Geological Association of Geological Societies Transactions, V.60; 133-148.

Dean, W.E. and Arthur, M.A., 1989. Iron-Sulfur-Carbon relationships in organic-carbon-rich sequences I Cretaceous Western Interior seaway, American Journal or Science, Vol. 289; 708-743.

Dean, W.E., Gardner, J.V., Piper, D.Z., 1997. Inorganic geochemical indicators of glacial-interglacial changes in productivity and anoxia on the California continental margin. Geochim. Cosmochim. Acta 61; 4507-4518.

Demiason, G.J. Moore, D.T., 1980. Anoxic environments and oil source bed genesis. AAPG Bull. 64; 1179-1209.

Dill, H., 1986. Metallogenesis of Early Paleozoic graptolite shales from the Graefenthal Horst (North Bavaria- Federal Republic of Germany). Econ. Geol. 81; 889-903.

Ewing, T.E., 1991. Structural framework, in A.Salvador, ed., The Gulf of Mexico Basin: Boulder, CO, Geologic Society of America, The Geology of North America, vol.J; 31-52.

Ewing, T.E., 2001. Review of Late Jurassic Depositional System and Potential Hydrocarbon Plays, Northern Gulf of Mexico Basin, Gulf Coast Association of Geological Societies Transactions, Volume L1, 2011.

Faucette, R.C, Ahr, W.M, 1984. Depositional and Diagenetic History of Upper Jurassic Haynesville Formation, Teague Townsite Field, Freestone County, Texas, The Jurassic of the Gulf Rim, Proceedings of the Third Annual Research Conference Gulf Coast Section Society of Economic Paleontologists and Mineralogists Foundation, Ventress,W.P.S, Bebout,D.G, Perkins,B.F, Moore, C.H.;103 – 120.

Frakes, L.A., Francis, J.E., Syktus, J.I., 1992. Climate Modes of the Phanerozoic. Cambridge University Press, Cambridge; 274.

Goldhammer, R.K., 1998. Second-order accommodation cycles and points of “stratigraphic turnaround”: Implications for carbonate buildup reservoirs in Mesozoic carbonate systems of the East Texas Salt Basin.

Goldhammer, R.K., 1999. Mesozoic sequence stratigraphy and paleogeographic evolution of northeast Mexico, Geological Society of America, Special Paper 340; 1-58.

Goldhammer, R.K., and C.A. Johnson, 1999. Middle Jurassic-Upper Cretaceous paloegeographic evolution and sequence-stratigraphic framework of the northwest Gulf of Mexico rim, in C.Bartolini, R.T. Buffler, and A.Canu-Chapa, eds., The western Gulf of Mexico Basin: Tectonics, sedimentary basin, and petroleum systems: AAPG Memoir 75; 45-81.

Hallam, A., 1978. Eustatic cycles in the Jurassic. Palaeogeogr. Palaeoclimatol. Palaeoecol. 23; 1-32.

Hallam, A., 1985. A review if Mesozoic climates. J. Geol. Soc. London 142; 433-445.

Hallam, A., 1988. A re-evaluation of Jurassic eustasy in the light of new data and the revised Exxon curve. In: Wilgus, C.K., Hastings, B.S., Kendall, C.G.St.C., Posamatir, H.W., Ron, C.A., van Wagner, J.C. (Eds.), Sea-Level Changes--An Integrated Approach. SEPM Special Publication, 42; 261-273.

Hallam, A., 2001. A review of the broad pattern of Jurassic sea-level changes and their possible causes in the light of current knowledge. Palaeogeogr. Palaeoclimatol. Palaeoecol. 167, 3-37.

Hammes, U., 2009. Sequence stratigraphy and core facies of the Haynesville Mudstone, east Texas: Gulf Coast Association of Geological Societies Transaction, v.59; 321-324.

Hammes, U., Hamlin, S.H., and Ewing, T., 2011. Geologic analysis of the Upper Jurassic Haynesville Shale in east Texas and west Louisiana, AAPG Bulletin, V.95, No.10; 1643-1666.

Haq, B.U., Hardenbol, J., Vail, P.R., 1987. Chronology of fluctuating sea levels since the Triassic (250 million years ago to present). Science 235; 1156-1167.

Jacobs, L., Emerson, S., Huested, S.S., 1987. Trace metal geochemistry on the Cariaco Trench: Deep-Sea Research, v.34; 965-981.

Jackson, M.L.W., and S. E. Laubach, 1988. Cretaceous and Tertiary Compressional tectonics as the cause of the Sabine Arch, East Texas and Northwest Louisiana, Transactions- Gulf Coast Association of Geological Societies, Volume XXXVIII.

Jenkyns, H.C., Schouten-Huibers, L., Schouten, S., Sinninghe-Damste, J.S., 2011. Middle Jurassic-Early Cretaceous high-latitude sea-surface temperatures from the Southern Ocean. Clim. Past Discuss, 7; 1339–1361.

Jones, B., Manning, D.A.C., 1994. Comparison of geochemical indices used for the interpretation of paleoredox conditions in ancient mudstones. Chem. Geol. 111; 111-129.

Kehle, R.O., 1971. Origin of the Gulf of Mexico: The University of Texas at Austin, Geology Library, Call no.q557K260, unpublished report, unpaginated.

Leventhal, J.S., 1983. An interpretation of carbon and sulfur relationships in Black Sea sediments as indicators of environments of deposition. Geochim. Cosmochim Acta 47; 133-138.

Li, Y. 1982. A brief discussion on the mean oceanic residence time of elements. Geochimica et Cosmochimica Acta. V. 46; 2671-2675.

Loucks, R.G., Ruppel, S.C., 2007. Mississippian Barnett Shale: Lithofacies and depositional setting of a deep-water shale gas succession in Fort Worth Basin, Texas, 2007. AAPG Bulletin, V.91, No.4; 579-601.

Lowrie, A., Sullivan, N.M., Krotzer, C., Carter, J., Lerche, I., and Petersen, K., 1993. Tectonic and Depositional model of the North Louisiana – South Arkansas Basin, Gulf Coast Association of Geological Societies.

Mancini, E.A., Puckett, T.M., and Parcell, W.C., 1999. Modeling of the Burial and Thermal Histories of Strata in the Mississippi Interior Salt Basin, Gulf Coast Association of Geological Societies Transactions, VOL. XLIX.

Mancini, E.A., Obid, J.A., and Puckett, T.A., 2004. Upper Jurassic Transgressive-Regressive Sequences, Mississippi Interior Salt Basin Area, Gulf Coast Association of Geological Societies Transactions, Volume 54; 415-424.

Marton, G.L., and R.T. Buffler, 1999, Jurassic-Early Cretaceous tectonopaleogeographic evolution of the southeastern Gulf of Mexico basin, in P. Mann, ed., Caribbean Basins : Sedimentary Basins of the World: Amsterdam, Elsevier Science B.V. v..4; 63-91.

McGowen and Harris, 1984. Depositional Systems in the East Texas Basin; The Jurassic of the Gulf Rim, Proceedings of the Third Annual Research Conference Gulf Coast Section Society of Economic Paleontologists and Mineralogists Foundation, Ventress,W.P.S, Bebout,D.G, Perkins,B.F, Moore, C.H.; 213 – 253.

Meyers, P.A., 1997. Organic geochemical proxies of paleoceanographic, paleolimnologic, and paleoclimatic processes, Permagon, Org. Geochem. Vol.276, No. 5/6; 213-250.

Moore, R.W., Del Castillo, L., 1974. Tectonic evolution of the southern Gulf of Mexico: Geological Society of America Bulletin, v. 85, no.4; 607-618.

Murphy, A.E., Sageman, B.B., Hollander, D.J., Lyons, T.L., Brett, C.E., 2000. Black shale deposition and faunal overturn in the Devonian Appalachian Basin: clastic starvation, seasonal water column mixing, and efficient biolimiting nutrient recycling Paleoceanography 15; 280-291.

Nunn, J.A., 1984. Subsidence and Temperature Histories For Jurassic Sediments in The Northern Gulf Coast : A Thermal-Mechanical Model, Proceedings of the Third Annual Research Conference Gulf Coast Section Society of Economic Paleontologists and Mineralogists Foundation, Ventress,W.P.S, Bebout,D.G, Perkins,B.F, Moore, C.H.; 309-322

Nunn, J.A., A.D. Scardina, and R.H. Pilger, Jr., 1984. Thermal Evolution of the north-central Tectonics, V.3; 723-740.

Orians, K.J., Bruland, K.W., 1986. The biogeochemistry of aluminum in Pacific Ocean. Earth Planet. Sci. Lett. 78; 397-410.

Peters, K.E., Sweeney, R.E. and Kaplan, I.R., 1978. Correlation of carbon and nitrogen stable isotope ratios in sedimentary organic matter. Limnology and Oceanography 23; 598-604.

Pearce, C. R., Coe, A.L., and Cohen, A.H., 2010. Seawater redox variations during the deposition of the Kimmeridge Clay Formation, United Kingdom (Upper Jurassic): Evidence from molybdenum isotopes and trace metal ratios, Paleoceanography, VOL.25, and PA4213.

Pilger, R.H., Jr., 1981. The opening of the Gulf of Mexico: implications for the tectonic evolution of the northern Gulf Coast: Gulf Coast Association of Geological Societies Transactions, v.31; 377-381.

Pindell, J.L., and Dewey, J.F., 1982. Permo-Triassic reconstruction of Western Pangea and the evolution of the Gulf of Mexico/Caribbean region: Tectonics, v.35; 251-260.

Pindell, J.L., and L. Kennan, 2009. Tectonic evolution of the Gulf of Mexico, Caribbean and northern South America in the mantle reference frame: an update: Geological Society of London Special publications 2009; v.328; 1-55.

Piper, D. Z. and Calvert. S.E., 2009. A marine biogeochemical perspective on black shale deposition, Elsevier, Earth Science Reviews 95; 63-96.

Pompeckj, J., 1901. Die Jura-Ablagerungen zwischen Regensburg and Regenstauf. (Ein Beitrag zur Kenntnis der Ostgrenze des Frankischen Jura). Geognistische Jahreshefte 14; 139-220.

Posamentier, H.W., Allen, G.P., 1999. Siliciclastic sequence stratigraphy – concepts and applications. SEPM (Society for Sedimentary Geology), Concepts in Sedimentology and Paleontology, No.7; 210

Prahl, F.G., Ertel. J.R., Goni, M.A., Sparrow, M.A. and Eversmeyer, B., 1994. Terrestrial organic carbon contributions to sediments on the Washington margin, Geochemica et Cosmochimica Acta 58; 3048-3055.

Pratt, L.M., Davis, C.L., 1992. Interwinded fates of metals, sulfur and organic carbon in black shales. In: Pratt, L.M., Comer, J.B., Brassell, S.C., (Eds.), Geochemistry of Organic Matter in Sediments and Sedimentary Rocks, SEPM Short Courses Notes, vol.27. Soc.Sed. Geol; 1-27.

Raiswell, R., Berner, R.A., 1986. Pyrite and organic matter in Phanerozoic normal marine shales: Geochimica et Cosmochimica Acta, V.50; 710-724.

Raiswell, R., Berner, R.A., 1987. Organic carbon losses during burial and thermal maturation of normal marine shales. Geology 15; 853-856.

Raiswell, R., Buckley, F., Berner, R.A., Anderson, T.F., 1988. Degree of pyritization of iron as a paleoenvironmental indicator of bottom water oxygenation. J. Sediment. Petrol. 58; 812-819.

Rau, G.H., Arthur, M.A., Dean, W.E., 1987. 15N/14N variations in Cretaceous Atlantic sedimentary sequences: implications for past changes in marine nitrogen biogeochemistry. Earth and Planetary Science Letters 82; 269-279.

Rimmer, S.M., 2004. Geochemical paleoredox indicators in Devonian-Mississippian black shales, Central Appalachian Basin (USA). Chemical Geology, 206; 373-391.

Rimmer, S.M., Thompson, J.A., Goodnight, S.A., Robl, T.L, 2004. Multiple controls on the preservation of organic matter in Devonian-Mississippian marine black shales: geochemical and petrographic evidence. Elsevier Publication, Paleogeography, Paleoclimatology, Paleoecology 215; 125-154.

Rowe, H.D., Loucks, R.G., Ruppel, S.C., and Rimmer, S.M., 2008. Mississippian Barnett Formation, Fort Worth Basin, Texas: Bulk geochemical inferences and Mo-TOC constraints on the severity of hydrographic restriction, Elsevier, Chemical Geology 257; 16-25.

Rowe, H.D., Mainali, P., (in review). Chemostratigraphy and Paleoceanography of the Late Jurassic Haynesville-Bossier System, East Texas Basin. AAPG Memoir.

Sageman, B.B, Murphy, A.E, Werne, J.P, Ver Straeten, C.A, Hollander, D.J and Lyons, T.W. 2003. A tale of shales: the relative roles of production in the accumulation of organic-rich strata, Middle-Upper Devonian, Appalachian basin. Chemical Geology 195; 229-273.

Sageman, B.B., Lyons, T.W., 2003. Geochemistry of fine-grained sediments and sedimentary rocks. In: MacKenzie, F. (Ed.), Treatise on Geochemistry 7. Elsevier Publishing; 115-158.

Salvador, A., 1987. Late Triassic-Jurassic paleogeography and origin of Gulf of Mexico basin, AAPG Bulletin 71; 419-451.

Salvador, A., 1991. The Gulf of Mexico Basin, Chapter 1. The Geology of North America , Vol J, The Gulf of Mexico Basin, The Geological Society of America; 1 - 12.

Schmitz, B., 1987. The TiO2/Al2O3 ratio in the Cenozoic Bengal abyssal fan sediments and its use as a palaeostream energy indicator. Mar. Geol. 76; 196-206.

Schudack, M.E., 1998. Ostracoda (marine/nonmarine) and paleoclimate history in the Upper Jurassic of Central Europe and North America, Marine Micropaleontology 37; 273-288.

Schieber, J., and W. Zimmerle, 1998, Introduction and overview: The history and promise of shale research, In: J. Schieber, W. Zimmerle, and P. Sethi (eds.), Shales and Mudstones I: Stuttgart, Germany, E. Schweizerhbart'sche Verlagsbuchhandlung; 1-10.

Scotese, C.R., Boucot, A.J., and Mckerrow, W.S., 1999. Gondwanan Paleogeography and Paleoclimatology, Permagon, Journal of African Earth Sciences, Vol. 28, No.1; 99-114.

Shimmield, G.B., 1992. Can sediment geochemistry record changes in coastal upwelling paleoproductivity? Evidence from northwest Africa and the Arabian Sea. In: Summerhayes, C.P., Prell, W.L., Emeis, K.C. (Eds.), Upwelling Systems: Evolution Since the Early Miocene, Geol. Soc. Spec. Publ., vol.64; 29-46.

Spain, D.R., and G.A. Anderson, 2010. Controls on Reservoir Quality and Productivity in the Haynesville Shale, Northwestern Gulf of Mexico Basin: Gulf of Geological Societies Transactions, v.60; 657-668.

Steinhoff, I., Cicero, A.D., Koepke, K. A., Dezelle, J., McClain, T., Gillett, C., 2011. Understanding the Regional Haynesville and Bossier Shale Depositional Systems in East Texas and Northern Louisiana: An integrated Structural/Stratigraphic Approach. Search and Discovery Article # 50379 (2011).

Stern, R. J., and Dickinson, W. R., 2010. The Gulf of Mexico is a Jurassic backarc basin, Geosphere, v.6; no.6; 739-754.

Taylor, S.P., Sellwood, B.W., 2002. The context of lowstand events in the Kimmeridgian (Late Jurassic) sequence stratigraphy evolution of the Wessex-Weald Basin, Southern England, Elsevier Publication, Sedimentary Geology 151; 89-106.

Tribovillard, N., Algeo, T.J., Lyons, T., Riboulleau, A., 2006. Trace metals as paleoredox and paleoproductivity proxies: An update, Elsevier, Chemical Geology 232; 12-32.

Twichell, S.C., Meyers, P.A., and Diester-Haass, L. 2002. Significance of high C/N ratios in organic-carbon-rich Neogene sediments under the Benguela Current upwelling system. Organic Geochemistry. 33; 715-722.

Tyson, R.V., Wilson, R.C.L., Downie, C., 1979. A stratified water column environmental model for the type Kimmeridge clay, Nature 277; 377– 380.

Vail, P.R., Mitchum, R.M. Jr., Thompson, S. III, 1977. Seismic stratigraphy and global changes of sea level, part 4: Global cycles of relative changes of sea level. In: Seismic Stratigraphy ± Applications to Hydrocarbon Exploration (C. E. Payton, ed.). Mem. Am. Ass. Petrol. Geol., 26; 83- 97.

Vail, P.R., Hardenbol, J., and Todd, R.G., 1984. Jurassic Unconformities, Chronostratigraphy and Sea-Level Changes from Seismic and Stratigraphy and Biostratigraphy, Proceedings of the Third Annual Research Conference Gulf Coast Section Society of Economic Paleontologists and Mineralogists Foundation, Ventress,W.P.S, Bebout,D.G, Perkins,B.F, Moore, C.H.; 347-364.

Ver Straeten, C.A., Brett, C.E., and Sageman, B.B., 2010. Mudrock sequence Stratigraphy: A multi-proxy (sedimentological, paleobiological, geochemical) approach, Devonian Appalachian Basin, Palaeogeography, Palaeiclimatology, Palaeoecology, Volume 204, Issue 1-2; 54-73.

Wedepohl, K.H., 1971. Environmental influences on the chemical composition of shales and clays. In: Ahrens, L.H., Press, F., Runcorn, S.K., Urey, H.C. (Eds.), Physics and Chemistry of the Earth vol. 8, Pergamon, Oxford (1971), pp. 305–333.

Werne, J.P., Sageman, B.B., Lyons, T. and Hollander, D.J. 2002. An Integrated Assessment of a “Type Euxinic” deposit: Evidence for Multiple controls on Black Shale Deposition in the Middle Devonian Oatka Creek Formation, American Journal of Science, Vol. 302; 110-143.

Wignall, P.B., Maynard, J.R., 1993. The sequence stratigraphy of transgressive black shales. Source Rocks in a Sequence Stratigraphic Framework, Katz, B.J., Pratt, L. (Eds.), AAPG Stud. Geol. 37; 35-47.

Wignall, P.B., and R. Newton, 2001. Black shales on the basin marine: a model based on examples from the Upper Jurassic of the Boulonnais, northern France, Sedimentary Geology 144; 335-356.

Wood, M.L., and Walper, J.L., 1974. The evolution of the interior western basins and the Gulf of Mexico: Gulf Coast Association of Geological Societies Transactions, v.24; 31- 41.

Zheng, Y., Anderson, R.F., Green, A. V., and Kuwabara, J, 2000. Authigenic molybdenum formation in marine sediments: A Link to pore water sulfide in the Santa Barbara Basin, Geochimica et Cosmochimica Acta, Vol.64, No.24; 4165-4178.

BIOGRAPHICAL INFORMATION

Pukar Mainali graduated with a B.S. in geology-engineering option from the University of Texas at Arlington in August 2009. Impressed by the curriculum and research work done at UT Arlington, he stayed for a Master's degree. He worked under the direction of Dr. Harold Rowe and studied shale geochemistry.